Dinh *et al. Int J Concr Struct Mater* (2025) 19:63
https://doi.org/10.1186/s40069-025-00804-1

International Journal of Concrete Structures and Materials

RESEARCH **Open Access**

# Evaluation of KDS 14 Draft Model for One-Way Shear Strength of Slender Concrete Members Reinforced with Fiber-Reinforced Polymer (FRP) Rebars

Ngoc Hieu Dinh[1], Si-Hyun Kim[1] and Kyoung-Kyu Choi[1*]

**Abstract**

Currently, the evaluation methods and design codes for predicting the shear strength of FRP-RC members are being continuously developed and updated. The revision draft of the Korean Standard KDS 14 20 22 (KDS 14 draft) adopts the compression zone failure mechanism theory to predict the one-way shear strength of slender steel-reinforced concrete members. This study extends the application of the KDS 14 draft model to slender concrete members reinforced with fiber-reinforced polymer (FRP) rebars. The model performance was evaluated using a comprehensive database of slender FRP-reinforced concrete (RC) specimens, including 304 and 110 specimens without and with FRP stirrups, respectively. The strength prediction of the KDS 14 draft model was compared with those of the existing state-of-the-art international design guidelines and of other recently developed models for FRP-RC members. The KDS 14 draft model demonstrated promising performance over a wide range of design parameters, exhibiting the lowest scatteredness among the evaluated methods. It exhibited a strong correlation with the dataset while maintaining an acceptable level of safety and reliability. Among the investigated design models, the ACI 440.11-22 design method exhibited the highest scatteredness and conservatism for specimens without FRP stirrups. However, the JSCE model provided overly conservative predictions for specimens with FRP stirrups because of the rigorous adoption of a strain limit for FRP stirrups. In addition, parametric analyses were conducted, and design examples were presented to further understand the influence of key design parameters and the applicability of the KDS 14 draft model for FRP-RC beams.

**Keywords** Fiber-reinforced polymer, One-way shear strength, Design codes, RC beams, Compression zone

## 1 Introduction

Fiber-reinforced polymer (FRP) reinforcement has gained significant attention in recent years as a viable alternative to traditional steel reinforcement in reinforced concrete (RC) members (Dinh et al., 2024; Park et al., 2021; Pham et al., 2023). The primary advantage of FRP materials lies in their inherent resistance to corrosion, effectively addressing the durability challenges associated with steel reinforcement, particularly in environments exposed to deicing salts or marine conditions, which are known to accelerate steel corrosion. This corrosion resistance not only improves the durability and longevity of structures but also significantly reduces long-term maintenance and replacement costs, contributing to overall economic and sustainability benefits. In addition, FRP rebars offer other significant benefits, such as being lightweight, high tensile strength, and exhibiting outstanding fatigue

Journal information: ISSN 1976-0485 / eISSN 2234-1315.

*Correspondence:
Kyoung-Kyu Choi
kkchoi@ssu.ac.kr
[1] School of Architecture, Soongsil University, 369 Sangdo-ro, Dongjak-gu, Seoul 153-743, South Korea

resistance (Dinh et al., 2023; Xue et al., 2016). These properties make FRP reinforcement an attractive choice for construction projects, as it can accelerate construction timelines and reduce labor costs due to its ease of handling, cutting, transportation, and installation.

From a structural perspective, FRP reinforcement exhibits high tensile strengths and are available at different stiffness levels and strengths, increasing their applicability in structural components, such as beams (Huang et al., 2021; Ruan et al., 2020), columns (Morgado et al., 2015), and slabs (Mohamed & Khattab, 2017). Unlike steel reinforcements, FRP rebars show linear elastic response up to failure without yielding, which may increase the potential for unexpected brittle shear failure modes in flexural members. Therefore, careful design and detailing are critical considerations when using FRP reinforcements (Michaluk et al., 1998; Kara, 2011).

Understanding one-way shear behavior is essential for structural design and assessment of slender concrete beams reinforced with FRP rebars. For example, Guadagnini (2002) comprehensively studied the shear mechanisms of FRP-reinforced concrete (FRP-RC) beams and reported that the strain developed in flexural and FRP shear reinforcements can significantly exceed the values prescribed by the current design codes for FRP-RC members. In addition, compared with steel-reinforced beams, FRP-reinforced beams exhibited a more pronounced increase in crack width as the load increased. This behavior reduced friction along the crack length, thereby diminishing aggregate interlock resistance. Similarly, Wegian and Abdalla (2005) conducted four-point bending tests to evaluate the shear resistance of concrete beams reinforced with carbon FRP and glass FRP. They demonstrated that FRP-RC displayed linear behavior up to the first cracking owing to the lower elastic moduli of FRP compared to steel bars, followed by a reduction in stiffness post-cracking. The shear resistance attributable to dowel action in FRP-RC elements was reduced by approximately 70% compared with that of steel-reinforced RC elements. El-Sayed et al., (2006a, 2006b) and Alam et al. (2011) further conducted experiments to assess the effects of the quantity and stiffness of FRP rebars on the shear strength of concrete beams. Their findings indicated that the behavior of concrete beams in the post-cracking stage was primarily influenced by the FRP axial stiffness, showing that the shear strength increased as the reinforcement ratio or elastic modulus of FRP reinforcement increased. Furthermore, a study by Alam et al. (2011) identified the linear relationship between the cubic root of axial stiffness of FRP reinforcement and the normalized shear strength. A more recent study conducted by Betschoga et al. (2021) explored the effect of different loading types (concentrated and uniformly distributed loads), and boundary conditions (simply supported and cantilever conditions) on the shear behavior of FRP-reinforced beams without stirrups. They reported that these parameters caused notable differences in the location of critical shear cracks and the ultimate shear strength. In addition, they developed a shear strength model for FRP-RC beams based on the critical shear band concept, which was validated against existing data.

Recent studies have been carried out to address the challenges of predicting the one-way shear strength of FRP-RC members. Mukhtar and Deifalla (2023) developed a critical shear crack-based model supported by an extensive test database, offering a reliable approach for predicting shear strength in deep FRP-RC beams. Rahal (2023) proposed a unified shear strength equation applicable to both slabs and beams reinforced with FRP or steel, leveraging simplified cracked elastic properties for practical design. Wakjira et al. (2022) employed explainable machine learning models to enhance shear capacity predictions, demonstrating the potential of data-driven techniques in capturing complex shear capacity of FRP-RC beams. Nguyen and Dang (2025) extended the beam and arch action model using data-driven analysis, improving shear strength estimates for FRP-RC deep beams. Similarly, Xue et al. (2025) refined predictions by focusing on the average ultimate strain in stirrups, emphasizing the role of reasonable strain assessment in enhancing accuracy.

For practical design and performance assessment, existing design provisions adopted empirical or semi-empirical equations to predict the one-way shear strength of slender FRP-RC members, as summarized in Table 1. These equations are typically based on those originally developed for steel-RC members and are calibrated using different experimental datasets. The recent ACI 440.11-22 (ACI, 2022) model is based on modification of the ACI 318-19 (ACI, 2019) model, which was originally developed for steel RC members. This design model calculates the shear contribution of concrete ($V_c$) in FRP-RC members by considering factors such as the longitudinal FRP reinforcement ratio ($\rho_{fl}$), square root of concrete compressive strength ($f'_c{}^{0.5}$), and modulus ratio between FRP reinforcement and concrete. In addition, the ACI 440.11-22 model also incorporates adjustments for the member depth size effect ($\lambda_s$) and accounts for the minimum shear strength contributed by the concrete. The JSCE (2007) design method stipulated by the Japan Society of Civil Engineering (JSCE)

**Table 1** Summary of one-way shear strength models for FRP-RC members

| Models | Shear strength equations for concrete contribution | Shear strength equations for stirrup contribution |
|---|---|---|
| ACI 440.11-22 (2022) | $V_c = \frac{2}{5}\sqrt{f'_c}\lambda\lambda_s b_w kd \geq V_{c,\min}$<br>$k = \sqrt{2\rho_f(E_{fl}/E_c) + (\rho_f E_{fl}/E_c)^2} - \rho_f E_{fl}/E_c,$<br>$\lambda_s = \sqrt{2/(1+0.004d)} \leq 1.0, V_{c,\min} = 0.067\sqrt{f_c\prime}bd$ | $V_{fv} = \frac{A_{fv}f_{fv}d}{s}$<br>$f_{fv} = 0.005E_{fv} \leq f_{fb}, f_{fb} = (0.05r_b/d_b + 0.3)f_{fvu}$ |
| JSCE (2007) | $V_c = \beta_d\beta_p f_{vcd} b_w d$<br>$\beta_d = \sqrt[4]{1000/d} \leq 1.5(d \text{ in mm}), \beta_p = (100\rho_{fl}E_{fl}/E_s)^{1/3} \leq 1.5,$<br>$f_{Vud} = 0.2(f_c\prime)^{1/3} \leq 0.72$ | $V_{fv} = \frac{A_{fv}E_{fv}\varepsilon_{fv}}{s}z$<br>$\varepsilon_{fv} = 10^{-4}\sqrt{f_{fmcd}\frac{\rho_{fl}E_{fl}}{\rho_{fv}E_{fv}}} \leq f_{fb}/E_{fv}, f_{fb} = (0.05r_b/d_b + 0.3)f_{fvu}$<br>$f_{mcd} = \left(\frac{h}{300}\right)^{-1/10} f_c\prime$ ($h$ is in mm) |
| CSA/S806-12 (2021) | $V_n = 0.05\lambda k_m k_s k_a\left(1 + (E_{fl}\rho_f)^{1/3}\right)(f_c\prime)^{1/3} b_w d_v$<br>$d_v = \max(0.9d,\ 0.72h)$<br>$k_m = (d/a)^{0.5} \leq 1, k_a = \begin{cases} 1.0 \text{ for } (a/d) \geq 2.5 \\ 2.5\,d/a \text{ for } (a/d) < 2.5 \end{cases}$<br>$k_s = \frac{750}{450+d} \leq 1(d \text{ is in mm}), 0.11\sqrt{f'_c}bd \leq V_n \leq 0.22\sqrt{f'_c}bd$ | $V_{fv} = \frac{A_{fv}f_{fv}d_v}{s}\cot\theta$<br>$f_{fv} = 0.005E_{fv} \leq f_{fb}, f_{fb} = 0.4f_{fvu}$<br>$\theta = 30 + 7000\varepsilon_1, \varepsilon_1 = \frac{M_f/d_v + V_f}{2E_{fl}A_{fl}}, 30^{\circ} \leq \theta \leq 60^{\circ}$ |
| KDS 14 draft (2024) | $V_c = \lambda k_s f_{te} b_w c_u\sqrt{1 + f_{cc}/f_{te}}$<br>$k_s = 0.75 \leq \sqrt[4]{300/d} \leq 1.1$<br>$c_u = (-n\rho_{fl} + \sqrt{(n\rho_{fl})^2 + 2n\rho_{fl}})d, n = E_{fl}/E_c, f_{te} = 0.2\sqrt{f_c\prime},$<br>$f_{cc} = \frac{M_{ud}}{b_w c(jd)}, M_{ud} = 0.75M_u \geq 1.5M_{cr}$ | $V_{fv} = \frac{A_{fv}f_{fv}d}{s}$<br>$f_{fv} = 0.005E_{fv} \leq f_{fv}$ |
| Tarawneh et al. (2024) | $V_c = 0.4\lambda(n_c\rho_{fl})^{1/3}\sqrt{f'_c}b_w d, n_c = E_{fl}/E_c$ | |

$f'_c$ = Concrete compressive strength

$b_w$, $d$, and $a$ = Web width, effective depth, and shear span of the beam, respectively

$\rho_{fl}$, $E_{fl}$, = Reinforcement ratio and elastic modulus of FRP longitudinal rebars, respectively

$A_{fv}$, $f_{fv}$ $E_{fv}$, $\rho_{fv}$, $\varepsilon_{fv}$, $s$ = Cross-sectional area, design tensile strength, elastic modulus, reinforcement ratio, effective strain, and spacing of FRP shear rebars, respectively

$E_s$, and $E_c$: Elastic modulus of steel and concrete, respectively

$f_{fb}$ = Tensile strength of the bent portion of FRP shear rebar

guidelines considers several factors, including the modulus ratio $(E_{fl}/E_s)^{1/3}$ between the longitudinal FRP and steel rebars, size effect, and cube root of concrete compressive strength. The CSA/S806-12 (CSA, 2021) design method of the Canadian Standard Association (CSA) is based on the modified compression field theory (Vecchio & Collins, 1986). This approach takes into account the effects of axial stiffness of longitudinal rebars ($E_{fl}$ $\rho_{fl}$), size effect, and effective shear depth ($d_v$).

The revision draft of the Korean Standard KDS 14 20 22 (2024) (KDS 14 draft) issued by the Korea Concrete Institute adopted the unified shear strength model originally developed by Park et al. (2006) and Choi et al. (2016) to evaluate the one-way shear of steel RC members. This model is based on the theory of compression zone failure mechanisms and demonstrates a strong correlation with a comprehensive database encompassing a wide range of design parameters (Choi et al., 2016). However, because the model was specifically developed for steel-RC beams, additional evaluation is required to determine its applicability to other types of reinforcements, such as FRP rebars.

To address this limitation, the present study evaluates the applicability of the KDS 14 draft model to predict the one-way shear strength of slender FRP-RC members. This evaluation was conducted based on a comprehensive database of FRP-RC specimens, both with and without shear reinforcement. The prediction performance of the KDS 14 draft model was compared with those in the existing state-of-the-art international design guidelines and of other design models recently developed for FRP-RC members. In addition, a parametric analysis and a design example were conducted to understand the influence of primary design parameters and the applicability of the KDS 14 draft model for FRP-RC beams.

## 2 Review of One-Way Shear Model Based on Compression Zone Failure Mechanism

In the KDS 14 draft model, the one-way shear of RC members carried by uncracked concrete is evaluated based on the compression zone failure mechanism (Choi et al., 2016). Fig. 1 depicts the shear resistance mechanism and stress state at the shear-critical section in the compression zone of slender RC beams. During the initial loading stage, multiple flexural cracks initiated in the tension zone of the beams. These flexural cracks propagated toward the web of the beam with an increase in the applied load, eventually reaching the compression zone and leading to the formation of critical shear cracks. At the ultimate stage, the compression zone (A-B zone) could no longer function as a continuum and became

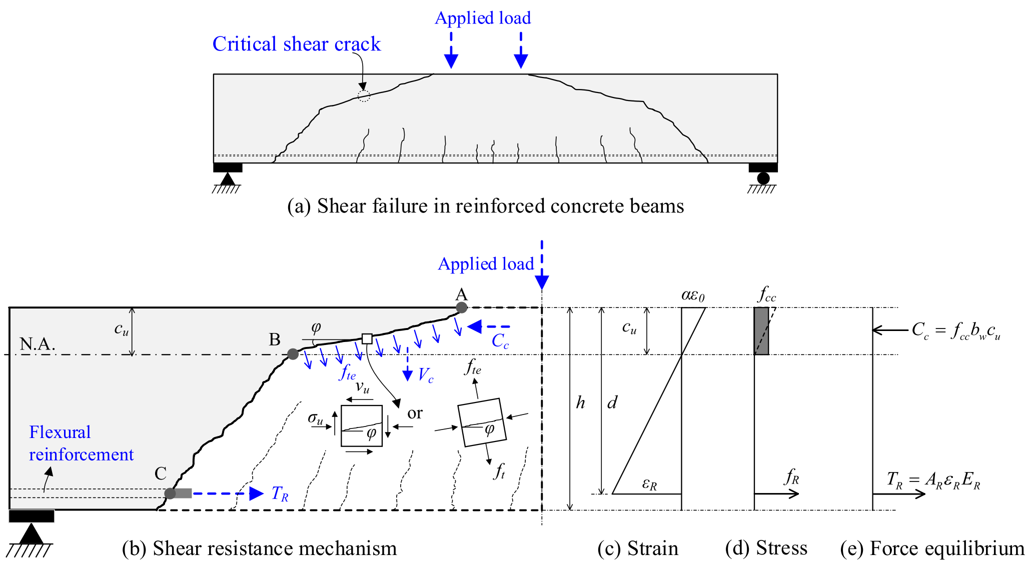


**Fig. 1** Shear resistance mechanism of reinforced concrete beams and force equilibrium and strain compatibility at the critical section (Choi et al., 2016)

incapable of resisting the compressive forces triggered by the applied flexural moment, which facilitated the occurrence of brittle shear failure (Choi et al., 2016; Dinh et al., 2020). The shear resistance capacity provided by the compression zone could be estimated as follows (Choi et al., 2016):

$$V_c = f_{te}\frac{c_u}{\sin\varphi}b_w\cos\varphi = f_{te}b_wc_u\cot\varphi \tag{1}$$

where $f_{te}$ [$=0.2\sqrt{f_c'}$] is the concrete tensile strength specified in the KDS 14 draft model; $c_u$ is the depth of the compression zone; $f_c\prime$ is the compressive strength of concrete; $b_w$ is the beam's web width, and $\varphi$ is the average angle of inclined crack in the compression zone, defined by the principal stress axis using the Rankine failure criterion:

$$\cot\varphi = \sqrt{f_{te}(f_{te}+f_{cc})}/f_{te} \tag{2}$$

where $f_{cc}$ = average compressive normal stress in the compression zone.

Substituting Eq. (2) into Eq. (1), the shear contribution of the compression zone is determined as:

$$V_c = f_{te}b_wc_u\sqrt{1+f_{cc}/f_{te}} \tag{3}$$

By considering the size effect factor ($k_s$) and reduction factor for lightweight concrete ($\lambda$), the final expression for $V_c$ in the KDS 14 draft model is given by:

$$V_c = \lambda k_s f_{te}b_wc_u\sqrt{1+f_{cc}/f_{te}} \tag{4}$$

where

$$k_s = 0.75 \le \sqrt[4]{300/d} \le 1.1 \tag{5}$$

$$\lambda = \begin{cases} 1 \text{ for normal weight concrete} \\ 0.85 \text{ for lightweight concrete} \end{cases} \tag{6}$$

In the actual design, the depth of the compression zone $c_u$ in Eq. (4) could be determined based on the conditions of force equilibrium and strain compatibility. As illustrated in Fig. 1c–e, these conditions can be expressed by assuming a linear distribution of compressive stress and strain in the compression zone:

$$C_c = T_R, \tag{7a}$$

or

$$\frac{1}{2}\alpha\varepsilon_0E_cb_wc_u = A_R\varepsilon_RE_R = \rho_Rb_wd\varepsilon_RE_R \tag{7b}$$

$$\varepsilon_R = \alpha\varepsilon_0(d-c_u)/c_u \tag{8}$$

where $\alpha$ is the ratio of the current compressive strain to compressive normal strain at extreme compression fiber; $T_R$ is the tensile force in the reinforcement; $C_c$ is the resultant compressive force in the compression zone; $A_R$ and $E_R$ is the total cross-sectional area and elastic modulus of the tensile reinforcement, respectively; $\rho_R$ is the longitudinal reinforcement ratio; $\varepsilon_0$ [≈ 0.002] is the compressive strain corresponding to the concrete compressive strength; and $\varepsilon_R$ is the strain in tensile reinforcement.

From Eqs. (7) and (8), the final equation for $c_u$ is obtained as

$$c_u = d(-n\rho_R + \sqrt{(n\rho_R)^2 + 2n\rho_R}) \tag{9}$$

where $n$ [$=E_R/E_c$] is the modulus ratio between the tensile reinforcement and concrete.

The one-way shear strength in the compression failure mechanism-based model was significantly influenced by the magnitude of the average compressive stress ($f_{cc}$) acting on the compression zone, as indicated in Eq. (4). Under a factored flexural moment ($M_u$) at a given design section, $f_{cc}$ can be directly calculated using the following equation (KDS 14 draft model, 2024):

$$f_{cc} = \frac{M_{ud}}{b_w c\,(jd)} \le \frac{2}{3} f'_c \tag{10}$$

where $M_{ud}[= 0.75M_u \geq 1.5M_{cr}]$ is the design-factored flexural moment for conservative design purposes, $jd$ [$=d$-$c_u$/3] is the moment arm, which is simply calculated assuming that compressive stress follows a linear distribution in the compression zone, and $M_{cr}$ is the cracking moment (ACI 318-19, 2019). It should be noted that in the KDS 14 draft design method, a lower limit of the flexural moment, set at $1.5M_{cr}$ in Eq. (10), is recommended. This accounts for the assumption in the compression zone failure theory (Choi et al., 2016) that significant damage in the tension zone is a prerequisite for the formation of inclined tensile cracking in the compression zone.

The design equations of the KDS 14 draft model are summarized in Table 1.

## 3 Evaluation of Design Provisions

### 3.1 Database of FRC-RC Specimens

A comprehensive database of concrete specimens reinforced with FRP rebars, obtained from one-way shear tests, was used to evaluate the applicability of the KDS 14 draft model. The dataset, detailed in the Appendix, comprised 304 specimens without FRP shear reinforcement (Table 2) and 110 specimens with stirrups (Table 3). It should be noted that the previous studies in the database reported two types of concrete compressive strength, from cylinder tests ($f'_c$) and cube tests ($f_{cu}$). The data presented in the database in the Appendix adopt a unified compressive strength as $f'_c$ using the conversion relationship $f'_c = 0.80 f_{cu}$ (Mosley, 1999).

Figs. 2 and 3 present the specimen number distribution in the database with respect to several design parameters. The database covered different types of FRP reinforcement: carbon FRP (CFRP), aramid FRP (AFRP), GFRP, and basalt FRP (BFRP).

In Fig. 2, the design parameters for FRP-RC specimens without stirrups are as follows: the axial stiffness of FRP reinforcement ($\rho_{fl}\ E_{fl}$) varied from 150 to 7174 MPa; the compressive strength of concrete ($f'_c$) ranged from 20 to 102 MPa; and the shear span-to-effective depth ratio ($a/d$) varied from 2.5 to 8.

In Fig. 3, the design parameters for FRP-RC specimens with stirrups are as follows: the concrete compressive strength ($f'_c$) ranged from 20 to 102 MPa; the shear span-to-effective depth ratio ($a/d$) ranged from 1.19 to 4.5; and the axial stiffness of FRP longitudinal reinforcement ($\rho_{fl}\ E_{fl}$) varied between 246 and 7174 MPa; and the axial stiffness of FRP stirrups ($\rho_{fv}\ E_{fv}$) varied between 38 to 1470 MPa.

In addition, the database included other parameters, such as cross-sectional shapes (rectangular, I-shaped, and T-shaped), concrete types (normal weight and lightweight), and effective depths ranging from 73 to 937 mm. Most specimens in the two datasets were reinforced with CFRP (113 specimens) and GFRP rebars (273 specimens). Fig. 4 illustrates the influence of key design parameters on the normalized one-way shear strength of FRP-RC beams in the database. It was shown that the axial stiffness of the FRP longitudinal rebar and the effective depth most significantly influenced the shear strength, whereas the concrete compressive strength and the ratio of shear span to effective depth ($a/d$) exerted a comparatively lower impact for slender beams with $a/d \geq 2.5$.

### 3.2 Shear Design Provisions

In this study, three existing state-of-the-art international design guidelines are used for a comparative analysis with the KDS 14 draft model: ACI 440.11-22 (2022) issued by the ACI Committee 440, JSCE (2007) issued by the JSCE, and CSA/S806-12 (2021) issued by the CSA. In addition, we used a unified shear design model recently developed by Tarawneh et al. (2024) for slender RC members. This model is based on modifications of the ACI 318-19 model to account for the axial stiffness of longitudinal reinforcement and exhibits promising performance in predicting the one-way shear of both steel-RC and FRP-RC members with and without shear reinforcement.

### 3.3 Shear Strength Evaluation Using the KDS 14 Draft Model and Comparison with Existing Design Methods

Tables 2 and 3 in the Appendix summarize the test results for the one-way shear strength of FRP-RC specimens without and with stirrups, respectively. It should be noted that for the evaluation process, material reduction, and safety factors in the design equations were set to 1.0 to ensure a consistent comparison. Statistical parameters, such as the minimum, maximum, and average values, coefficient of variation (COV), and average absolute error (AAE) of the shear strength ratio between test and prediction results, were used to evaluate the reliability of design models. The AAE was calculated using Eq. (11) as follows:

$$\mathrm{AAE} = \frac{1}{n}\sum_{i=1}^{n}\left|\frac{V_{predict,i} - V_{test,i}}{V_{test,i}}\right| \quad (11)$$

where $n$ is the number of test specimens used in the statistics, and $V_{test,i}$ and $V_{predict,I}$ is the test results and predictions, respectively. AAE is one of the key statistical measures indicating the correlation between the dataset of prediction and test results: the lower the AAE value, the better the model correlates with the dataset. In addition, the safety of different design equations was assessed using the 5% fractal indicator ($P_{0.05}$), assuming a normal distribution of the ratio $V_{test}/V_{predict}$. The $P_{0.05}$ value is generally accepted as a characteristic value of resistance in the limit state theory (EN1990:2002, 2002): the closer the 5% fractal value closer to 1, the better the safety. In addition, the figures report the percentage of specimens with $V_{test}/V_{predict}$ less than 0.75, which corresponds to the strength reduction factor for shear design.

For the application of the KDS 14 draft model to the existing database, the elastic modulus ($E_{fl}$) and longitudinal reinforcement ($\rho_{fl}$) for FRP rebars were substituted for $E_R$ and $\rho_R$ values in design Eqs. (7–9). In addition, according to the KDS 14 draft model, the one-way shear strength of concrete ($V_c$) varied along the member length because of the variation in the average compressive stress ($f_{cc}$) caused by the factored flexural moment (Eq. 10). Therefore, $V_c$ should be checked along the member length at the potential shear-critical sections during the design process. For most specimens in the database, which were simply supported and subjected to four-point bending, the KDS 14 draft model recommends checking the location of the critical shear section at a distance of 1.2 times the effective depth from the end support. Therefore, the designed factored flexural moment ($M_{ud}$) in Eq. (10) can be calculated using $[M_{ud} = (1.2\,d)V_{test} \geq 1.5M_{cr}]$, where $V_{test}$ is the shear load at failure obtained from test results.

#### *3.3.1 FRP-RC Specimens Without Stirrups*

Fig. 5 presents the distribution of the shear strength ratio $V_{test}/V_{predict}$ according to the axial stiffness of FRP longitudinal rebars and the effective depth for FRP-RC specimens without stirrups. Overall, all prediction models provided conservative estimations when compared to the experimental results across different design parameters. For all prediction models, the percentage of specimens with $V_{test}/V_{predict}$ ratios below 0.75 was minimal, ranging from 0% to 1.32%.

Among the models, ACI 440.11-22 (Fig. 5b) exhibited the highest scatteredness, with a COV of 22% and the highest conservatism compared to the experimental data, reflected in a mean value of $V_{test}/V_{predict}$ of 1.71 and a $P_{0.05}$ value of 1.38. Compared to other models, the prediction results of the KDS 14 draft model (Fig. 5a) exhibited the lowest scatteredness, with a COV value of 20% and good correlation with the test results, as evidenced by a mean $V_{test}/V_{predict}$ ratio of 1.29 and AAE of 0.22. In addition, the KDS 14 draft model yielded a $P_{0.05}$ value close to 1.0, indicating an acceptable level of safety and reliability.

Compared to the KDS 14 draft model, the empirical model proposed by Tarawneh et al. (2024) (Fig. 5e) yielded a similar performance, whereas the JSCE model (Fig. 5c) displayed slightly higher variability and mean strength ratios. Although the CSA/S0806 model (Fig. 5d) exhibited a good correlation with test results, with a mean $V_{test}/V_{predict}$ ratio of 1.17 and an AAE of 0.18, it displayed a lower safety level compared to other models, with a $P_{0.05}$ value of 0.74.

#### *3.3.2 FRP-RC Specimens with Stirrups*

Fig. 6 shows the distribution of the shear strength ratio $V_{test}/V_{predict}$ according to the FRP shear reinforcement ratio ($\rho_v$) and the effective depth for FRP-RC specimens with stirrups. The shear reinforcement ratio was calculated as $[A_{fv}/b_w s]$, where $A_{fv}$ is the area of the FRP shear reinforcement ratio within the spacing $s$. Table 1 summarizes the shear strength equations for stirrup contributions for different design codes. Generally, in all design models, the shear contribution of FRP reinforcement is expressed as

$$V_{fv} = \frac{A_{fv} f_{fv} d_v}{s} \cot \theta \quad (12)$$

where $f_{fv}$ is the effective tensile strength of FRP reinforcement used for shear design, $\theta$ is the inclination angle of the diagonal concrete strut, and $d_v$is the effective shear depth.

As shown in Table 1, the primary differences between design codes for calculating $V_{fv}$ concern the effective tensile strength of FRP stirrups and the inclination angle of the diagonal concrete strut. Considering that FRP exhibited linear behavior up to failure, different codes prescribed varying strain limits for FRP stirrups to control the crack width (Tarawneh et al., 2024). The ACI 440.11-22 and CSA/S806 models adopted the design strength of FRP stirrups corresponding to a strain limit of 0.005 or a strength limit based on the tensile strength of the bent portion of FRP stirrups ($f_{fb}$). In contrast, the JSCE model specifies a more conservative strain limit of FRP stirrups, considering the axial stiffness ratio between longitudinal ($\rho_{fl}E_{fl}$) and shear ($\rho_{fv}E_{fv}$) reinforcement, as well as concrete compressive strength. In addition, the CSA/S806 model adopted an empirical equation based on the MCFT to determine the inclination angle of the diagonal concrete strut, which was different from the value of 45° used in the ACI 440.11-22 and JSCE models. The KDS 14 draft model for steel reinforcement adopted the same design equation as ACI 318-19 (ACI, 2019) for stirrup shear contribution. Therefore, we adopted the same shear strength equation for FRP stirrup contributions using the ACI 440.11-22 method.

The prediction results of the KDS 14 draft model (Fig. 6a) exhibited the lowest scatteredness, with a COV value of 22%, and displayed the best correlation with test results, as represented by a mean $V_{test}/V_{predict}$ ratio of 1.18 and an AAE of 0.2. The percentage of specimens with $V_{test}/V_{predict}$ ratios below 0.75 predicted by the KDS 14 draft model was relatively small, within an acceptable level (2.73%). The ACI 440.11-22 and CSA/S0806 (Fig. 6b & c) yielded similar performances with mean $V_{test}/V_{predict}$ ratios of 1.52–1.54, COVs of 25–27%, and AAEs of 0.32–0.33. The model by Tarawneh et al. (Fig. 6e) maintained a balance between safety and reasonable correlation with the experimental dataset. In particular, the JSCE model (Fig. 6d) displayed overly conservative predictions reflected in a mean value of $V_{test}/V_{predict}$ of 2.62 and very high scatteredness (COV of 30%). This is attributed to the fact that the JSCE model adopted an excessively conservative strain limit for FRP stirrups, thereby underestimating the shear contribution of stirrups.

## 4 Parametric Study Using Design Models

Fig. 7 shows the parametric study results using the KDS 14 draft and existing design models to understand the influence of primary parameters on the one-way shear strength of concrete beams reinforced with FRP bars. The effect of the effective depth of the beam is shown in Fig. 7a. The effective depth of analytical beams varied from 0.15 to 0.55 m, whereas that of other design parameters was similar to that examined by Ashour and Kara (2014). For all design models, the anticipated shear strength increased proportionally with the effective depth of the beams. In the KDS 14 draft model, an increase in the effective depth increased the compression zone depth (Eq. 9), which, consequently, enhanced the shear strength. An analogous increasing tendency of shear strength was observed (Fig. 7b) as the concrete compressive strength increased from 20 to 90 MPa. This phenomenon is attributed to the increase in compressive strength that increases the tensile strength of the concrete and contributes to the overall shear resistance of the compression zone (Eq. 1).

The influence of axial stiffness of FRP longitudinal rebars ($\rho_{fl}$ $E_{fl}$) is shown in Fig. 7c. The analytical beams used $\rho_{fl}$ $E_{fl}$ varied from 202 to 968 MPa by increasing the FRP reinforcement ratio from 0.5% to 2.4%. Higher axial stiffness led to higher shear strength prediction because the KDS 14 draft model determined the compression zone depth considering the effect of FRP axial stiffness, as shown in the Eqs. (7)–(9) for force equilibrium and strain compatibility. A similar increasing trend in shear strength is observed with an increase in the shear reinforcement ratio, as shown in Fig. 7d, due to the enhanced contribution of stirrups to the overall shear strength.

Overall, the parametric study presented in Fig. 7 indicates that one-way shear strength predictions by the KDS 14 draft model exhibited a similar trend to the state-of-the-art design methods for FRP-RC beams, which were conservative and consistent with the test results in several current studies (Alam, 2010; Ashour & Kara, 2014; Johnson, 2014; Yost et al., 2001).

## 5 Design Example

To understand the KDS 14 draft methods, a design example was provided for a fixed-end concrete beam reinforced with FRP rebars and subjected to a uniformly distributed load of $w_u$=100 kN/m (including the self-weight), as presented in Fig. 8. The beam had a span length of $L$=8 m and cross-sectional dimensions of $b\times d$=0.4×0.6 m. The beam used normal-weight concrete with $f'_c$=27 MPa and GFRP bars as longitudinal and shear reinforcements with $f_{fu}^*$=700 MPa and $E_f$=47.5 GPa. The longitudinal reinforcement ratio was $\rho_{fl}$=1.02% (5Φ25), whereas the shear reinforcement ratio was $\rho_{fv}$=0.39% (Φ10@100 mm) within two lengths of $L/4$ from the support end and $\rho_{fv}$=0.26% (Φ10@150 mm) in the remaining span.

Assuming interior exposure conditions for the design process, the designed tensile strength of GFRP bars was calculated as $f_{fu}=C_e\ f_{fu}^*$=(0.8) (700)=560 MPa. Shear strengths were calculated and checked at several cross sections: $A_1$ within the shear span (at a distance $d$ from the support end) and ($A_2$–$A_3$) outside the shear span. Fig. 8b and c shows the factored moment and shear force distributions, respectively.

The representative calculation at cross-section $A_1$ following the KDS 14 draft design method is as follows:

- Calculation of the compression zone depth:

$$n = E_f/E_c = 47,500/(4700\sqrt{27}) = 1.945$$

$$c_u = d\left(-n\rho_f + \sqrt{(n\rho_f)^2 + 2n\rho_f}\right) = 0.6\left(-0.0199 + \sqrt{(0.0199)^2 + 2\times 0.0199}\right) = 0.108\,\text{m}$$

- Calculation of the compression zone crack angle:

$$M_{ud} = 0.75M_u = 163.5\,\text{kNm} \geq 1.5M_{cr} = 157.8\,\text{kNm}$$

$$f_{cc} = \frac{M_{ud}}{b_w c_u\,(jd)} = \frac{157.8}{0.4(0.108)(0.6-0.108/3)} = 6.69\,\text{MPa} \leq \frac{2}{3}f'_c = 18\,\text{MPa}$$

$$\cot\varphi = \sqrt{1 + f_{cc}/f_{te}} = \sqrt{1 + 6.69/(0.2\sqrt{27})} = 2.73$$

- Calculation of shear contribution by concrete and FRP shear reinforcement:

$$k_s = \sqrt[4]{300/d} = 0.841 \rightarrow 0.75 \leq k_s \leq 1.1$$

$$V_c = \lambda k_s f_{te} b_w c_u \cot\varphi = 1\,(0.841)(1.04)(0.4)(0.108)(2.73) = 103\,\text{kN}$$

$$f_{fv} = 0.005E_{fv} = 238\,\text{MPa} < f_{fv} = 560\,\text{MPa}$$

$$V_{fv} = \frac{A_{fv}f_{fv}d}{s} = \rho_{fv}b_w d f_{fv} = 0.0039(0.4)(0.6)238 = 224\,\text{kN}$$

- Calculation of shear strength at cross-section $A_1$ and checking the condition:

$\phi V_n\,(\text{at A}_1) = \phi(V_c + V_{fv}) = 0.75\,(103 + 224) = 245\,\text{kN} > V_u = 238\,\text{kN}$. Thus, the beam satisfied the safety conditions.

We used the same calculation process to express the shear strengths at cross-section $A_2$ according to the KDS 14 draft design method and safety conditions as follows:

$\phi V_n\,(\text{at A}_2) = \phi(V_c + V_{fv}) = 0.75\,(58 + 149) = 208\,\text{kN} > V_u = 140\,\text{kN}$. Thus, the beam satisfied the safety conditions.

## 6 Conclusion

This study evaluated the applicability of the KDS 14 draft design method to predict the one-way shear strength of slender concrete members reinforced with FRP rebars. The evaluation was conducted using a large dataset of FRP-RC members, including 304 specimens without FRP stirrups and 110 specimens with FRP stirrups. The performance of the KDS 14 draft model was compared with that of state-of-the-art design codes and an empirical design model recently developed by Tarawneh et al. (2024). In addition, a parametric study analysis was conducted, and a design example was presented to investigate the influence of primary design parameters and the applicability of the KDS 14 draft design method for FRP-RC beams. The main conclusions are as follows:

1. The KDS 14 draft model demonstrated promising performance in predicting the one-way shear strength of a large dataset of slender FRP-RC members without FRP stirrups. It exhibited the lowest scatteredness compared to other current design methods, with a COV value of 20%. In addition, the model correlated well with the dataset, presented by a mean shear strength ratio of 1.29 and AAE of 0.22. The KDS 14 draft design method provided an acceptable level of safety and reliability, with a $P_{0.05}$ value of 0.86. The ACI 440.11-22 design method exhibited the highest scatteredness and conservatism, with a mean shear strength ratio of 1.71 and a $P_{0.05}$ value of 1.38.
2. For FRP-RC members with FRP stirrups, different design codes adopted different strain limits for FRP reinforcement to calculate the shear contribution of FRP stirrups. Compared to other methods, prediction results of the KDS 14 draft model exhibited the lowest scatteredness, with a COV value of 22%, and displayed the best correlation with the test results, as represented by a mean shear strength ratio of 1.18 and an AAE of 0.2. In addition, the percentage of specimens with shear strength ratios below 0.75 was relatively low (2.73%), indicating an acceptable level of safety. Overall, compared with the experimental dataset, all existing design methods yielded conservative predictions. In particular, the JSCE model displayed overly conservative predictions owing to the adoption of an excessively conservative strain limit for FRP stirrups.
3. A parametric study was conducted to examine the primary design parameters affecting the one-way shear strength of FRP-RC members, including the beam's effective depth, concrete compressive strength, axial stiffness of FRP longitudinal reinforcement, and shear reinforcement ratio. Overall, the KDS 14 draft model predictions exhibited a trend similar to that of the state-of-the-art design methods for FRP-RC beams, which were conservative and consistent with the test results in previous studies. In the KDS 14 draft model, increases in effective depth, concrete compressive strength, and FRP axial stiffness increased the compression zone depth determined by force equilibrium and strain compatibility conditions, leading to enhance the overall one-way shear strength.
4. The anticipated shear strength in the KDS 14 draft model, which is based on the compression zone failure theory, displayed a proportional increase in the effective depth of the beams due to increased compression zone depth. A similar tendency was observed with an increase in the concrete compressive strength, which was attributed to the improved tensile strength of concrete, thereby contributing to the overall shear resistance in the compression zone. Furthermore, the axial stiffness of FRP longitudinal rebars significantly affected the one-way shear strength of concrete members. Higher axial stiffness resulted in higher shear strength prediction owing to the improved compression zone depth.

**Table 2** Database of FRP-RC beams without FRP shear reinforcement

| Authors | Specimen | Cross-section | $L$ (m) | $b_w$ (m) | $h$ (m) | $d$ (m) | $a/d$ | $f'_c$ (MPa) | Concrete type | FRP type | $f_{fu}$ (MPa) | $E_f$ (GPa) | $\rho_f$ (%) | $V_{c,test}$ (kN) | $V_{c,KDS}$ (kN) | $V_{c,test}/V_{c,KDS}$ |
|---|---|---|---|---|---|---|---|---|---|---|---|---|---|---|---|---|
| Yost et al., (2001) | 1FRP | R | 2.13 | 0.23 | 0.29 | 0.23 | 4.10 | 36 | NW | GFRP | 690 | 40.3 | 1.11 | 39.1 | 32.7 | 1.20 |
| | 2FRP | R | 2.13 | 0.18 | 0.29 | 0.23 | 4.10 | 36 | NW | GFRP | 690 | 40.3 | 1.42 | 32.5 | 27.1 | 1.20 |
| | 3FRP | R | 2.13 | 0.23 | 0.29 | 0.23 | 4.10 | 36 | NW | GFRP | 690 | 40.3 | 1.65 | 45.4 | 36.3 | 1.25 |
| | 4FRP | R | 2.13 | 0.28 | 0.29 | 0.23 | 4.10 | 36 | NW | GFRP | 690 | 40.3 | 1.81 | 46.5 | 45.4 | 1.02 |
| | 5FRP | R | 2.13 | 0.25 | 0.29 | 0.23 | 4.10 | 36 | NW | GFRP | 690 | 40.3 | 2.05 | 46.2 | 42.7 | 1.08 |
| | 6FRP | R | 2.13 | 0.23 | 0.29 | 0.23 | 4.10 | 36 | NW | GFRP | 690 | 40.3 | 2.27 | 43.2 | 39.5 | 1.09 |
| El-Sayed et al. (2005) | S-C1 | R | 2.50 | 1.00 | 0.20 | 0.17 | 6.06 | 40 | NW | CFRP | 1536 | 114.0 | 0.39 | 143.8 | 106.7 | 1.35 |
| | S-C2B | R | 2.50 | 1.00 | 0.20 | 0.17 | 6.06 | 40 | NW | CFRP | 1536 | 114.0 | 0.78 | 170.8 | 128.4 | 1.33 |
| | S-C3B | R | 2.50 | 1.00 | 0.20 | 0.16 | 6.21 | 40 | NW | CFRP | 1536 | 114.0 | 1.17 | 193.8 | 142.4 | 1.36 |
| | S-G1 | R | 2.50 | 1.00 | 0.20 | 0.16 | 6.17 | 40 | NW | GFRP | 597 | 40.0 | 0.86 | 116.8 | 99.4 | 1.17 |
| | S-G2 | R | 2.50 | 1.00 | 0.20 | 0.16 | 6.29 | 40 | NW | GFRP | 540 | 40.0 | 1.70 | 145.8 | 118.9 | 1.23 |
| | S-G2B | R | 2.50 | 1.00 | 0.20 | 0.16 | 6.17 | 40 | NW | GFRP | 597 | 40.0 | 1.71 | 166.8 | 119.4 | 1.40 |
| | S-G3 | R | 2.50 | 1.00 | 0.20 | 0.16 | 6.29 | 40 | NW | GFRP | 540 | 40.0 | 2.44 | 166.8 | 130.9 | 1.27 |
| | S-G3B | R | 2.50 | 1.00 | 0.20 | 0.15 | 6.49 | 40 | NW | GFRP | 597 | 40.0 | 2.63 | 171.8 | 132.9 | 1.29 |
| El-Sayed et al., (2006a) | CN-1 | R | 2.75 | 0.25 | 0.40 | 0.33 | 3.07 | 50 | NW | CFRP | 1536 | 128.0 | 0.87 | 79.7 | 65.7 | 1.21 |
| | GN-1 | R | 2.75 | 0.25 | 0.40 | 0.33 | 3.07 | 50 | NW | GFRP | 608 | 39.0 | 0.87 | 72.7 | 47.9 | 1.52 |
| | CN-2 | R | 2.75 | 0.25 | 0.40 | 0.33 | 3.07 | 45 | NW | CFRP | 986 | 134.0 | 1.24 | 106.2 | 70.3 | 1.51 |
| | GN-2 | R | 2.75 | 0.25 | 0.40 | 0.33 | 3.07 | 45 | NW | GFRP | 754 | 42.0 | 1.22 | 62.2 | 51.4 | 1.21 |
| | CN-3 | R | 2.75 | 0.25 | 0.40 | 0.33 | 3.07 | 44 | NW | CFRP | 986 | 134.0 | 1.72 | 126.7 | 82.1 | 1.54 |
| | GN-3 | R | 2.75 | 0.25 | 0.40 | 0.33 | 3.07 | 44 | NW | GFRP | 754 | 42.0 | 1.71 | 79.7 | 55.8 | 1.43 |
| | CH-1.7 | R | 2.75 | 0.25 | 0.40 | 0.33 | 3.07 | 63 | NW | CFRP | 769 | 135.0 | 1.71 | 132.2 | 88.6 | 1.49 |
| | GH-1.7 | R | 2.75 | 0.25 | 0.40 | 0.33 | 3.07 | 63 | NW | GFRP | 754 | 42.0 | 1.71 | 89.2 | 63.7 | 1.40 |
| | CH-2.2 | R | 2.75 | 0.25 | 0.40 | 0.33 | 3.07 | 63 | NW | CFRP | 769 | 135.0 | 2.20 | 176.2 | 106.6 | 1.65 |
| | GH-2.2 | R | 2.75 | 0.25 | 0.40 | 0.33 | 3.07 | 63 | NW | GFRP | 754 | 42.0 | 2.20 | 117.7 | 68.1 | 1.73 |
| El-Sayed et al. (2009) | G1 | R | 4.50 | 0.60 | 0.30 | 0.26 | 6.68 | 68 | NW | GFRP | 683 | 48.0 | 0.77 | 89.2 | 105.1 | 0.85 |
| | G2 | R | 4.50 | 0.60 | 0.30 | 0.26 | 6.68 | 68 | NW | GFRP | 683 | 48.0 | 1.53 | 116.2 | 126.3 | 0.92 |
| Ashour (2006) | Beam 1 | R | 2.00 | 0.15 | 0.20 | 0.18 | 3.70 | 28 | NW | GFRP | 650 | 38.0 | 0.45 | 13.0 | 11.0 | 1.18 |
| | Beam 3 | R | 2.00 | 0.15 | 0.25 | 0.22 | 3.03 | 28 | NW | GFRP | 705 | 32.0 | 0.71 | 18.1 | 14.5 | 1.25 |
| | Beam 5 | R | 2.00 | 0.15 | 0.30 | 0.24 | 2.78 | 28 | NW | GFRP | 705 | 32.0 | 0.86 | 25.8 | 17.8 | 1.45 |
| | Beam 7 | R | 2.00 | 0.15 | 0.20 | 0.18 | 3.70 | 49 | NW | GFRP | 705 | 32.0 | 1.39 | 18.0 | 17.4 | 1.03 |
| | Beam 9 | R | 2.00 | 0.15 | 0.25 | 0.22 | 3.03 | 49 | NW | GFRP | 705 | 32.0 | 1.06 | 28.1 | 19.8 | 1.42 |
| | Beam 11 | R | 2.00 | 0.15 | 0.30 | 0.24 | 2.78 | 49 | NW | GFRP | 705 | 32.0 | 1.15 | 30.8 | 23.6 | 1.31 |
| Tureyen and Frosch (2002) | V-G1-1 | R | 2.44 | 0.46 | 0.41 | 0.36 | 3.40 | 35 | NW | GFRP | 606 | 40.5 | 0.96 | 108.1 | 79.7 | 1.36 |
| | V-G2-1 | R | 2.44 | 0.46 | 0.41 | 0.36 | 3.40 | 35 | NW | GFRP | 593 | 37.9 | 0.96 | 94.7 | 78.2 | 1.21 |
| | V-A-1 | R | 2.44 | 0.46 | 0.41 | 0.36 | 3.40 | 35 | NW | BFRP | 1420 | 47.1 | 0.96 | 114.8 | 83.0 | 1.38 |
| | V-G1-2 | R | 2.44 | 0.46 | 0.43 | 0.36 | 3.40 | 35 | NW | GFRP | 606 | 40.5 | 1.92 | 137.0 | 100.3 | 1.37 |

**Table 2** (continued)

| Authors | Specimen | Cross-section | $L$ (m) | $b_w$ (m) | $h$ (m) | $d$ (m) | $a/d$ | $f'_c$ (MPa) | Concrete type | FRP type | $f_{fu}$ (MPa) | $E_f$ (GPa) | $\rho_f$ (%) | $V_{c,test}$ (kN) | $V_{c,KDS}$ (kN) | $V_{c,test}/V_{c,KDS}$ |
|---|---|---|---|---|---|---|---|---|---|---|---|---|---|---|---|---|
| | V-G2-2 | R | 2.44 | 0.46 | 0.43 | 0.36 | 3.40 | 35 | NW | GFRP | 593 | 37.9 | 1.92 | 152.6 | 98.5 | 1.55 |
| | V-A-2 | R | 2.44 | 0.46 | 0.43 | 0.36 | 3.40 | 35 | NW | BFRP | 1420 | 47.1 | 1.92 | 177.0 | 104.4 | 1.69 |
| Razaqpur et al.(2004) | BR1 | R | 2.00 | 0.20 | 0.25 | 0.23 | 2.67 | 41 | NW | CFRP | 2250 | 145.0 | 0.25 | 37.0 | 25.2 | 1.47 |
| | BR2/ BA2 | R | 2.00 | 0.20 | 0.25 | 0.23 | 2.67 | 49 | NW | CFRP | 2250 | 145.0 | 0.50 | 47.9 | 32.4 | 1.48 |
| | BR3 | R | 2.00 | 0.20 | 0.25 | 0.23 | 2.67 | 41 | NW | CFRP | 2250 | 145.0 | 0.63 | 48.1 | 32.9 | 1.46 |
| | BR3 | R | 2.00 | 0.20 | 0.25 | 0.23 | 2.67 | 41 | NW | CFRP | 2250 | 145.0 | 0.88 | 43.6 | 35.4 | 1.23 |
| | BA3 | R | 2.00 | 0.20 | 0.25 | 0.23 | 3.56 | 41 | NW | CFRP | 2250 | 145.0 | 0.50 | 47.8 | 30.9 | 1.55 |
| | BA4 | R | 2.00 | 0.20 | 0.25 | 0.23 | 4.50 | 41 | NW | CFRP | 2250 | 145.0 | 0.50 | 39.2 | 30.3 | 1.29 |
| Zhao et al. (1995) | #1 | R | 1.80 | 0.15 | 0.30 | 0.25 | 3.00 | 34 | NW | CFRP | 1124 | 105.0 | 1.51 | 45.6 | 31.7 | 1.44 |
| | #6 | R | 1.80 | 0.15 | 0.30 | 0.25 | 3.00 | 34 | NW | CFRP | 1124 | 105.0 | 3.02 | 46.6 | 38.3 | 1.22 |
| | #15 | R | 1.80 | 0.15 | 0.30 | 0.25 | 3.00 | 34 | NW | CFRP | 1124 | 105.0 | 2.27 | 41.1 | 33.8 | 1.22 |
| Alkhrdaji et al. (2001) | BM7 | R | 1.50 | 0.18 | 0.33 | 0.28 | 2.69 | 24 | NW | GFRP | 717 | 40.0 | 2.30 | 54.0 | 32.0 | 1.69 |
| | BM8 | R | 1.50 | 0.18 | 0.33 | 0.29 | 2.61 | 24 | NW | GFRP | 717 | 40.0 | 0.77 | 36.6 | 21.8 | 1.68 |
| | BM9 | R | 1.50 | 0.18 | 0.33 | 0.29 | 2.61 | 24 | NW | GFRP | 717 | 40.0 | 1.34 | 40.6 | 25.3 | 1.61 |
| Tariq et al. (2003) | G07N | R | 2.50 | 0.16 | 0.38 | 0.35 | 2.75 | 37 | NW | GFRP | 674 | 42.0 | 0.72 | 60.3 | 26.8 | 2.25 |
| | G10N | R | 2.50 | 0.16 | 0.38 | 0.35 | 3.32 | 43 | NW | GFRP | 674 | 42.0 | 1.10 | 45.1 | 29.9 | 1.51 |
| | G15N | R | 2.50 | 0.16 | 0.38 | 0.33 | 3.54 | 34 | NW | GFRP | 674 | 42.0 | 1.54 | 47.8 | 30.2 | 1.58 |
| | C07N | R | 2.50 | 0.13 | 0.38 | 0.31 | 3.06 | 37 | NW | CFRP | 1506 | 120.0 | 0.72 | 48.5 | 27.7 | 1.75 |
| | C10N | R | 2.50 | 0.13 | 0.38 | 0.31 | 3.71 | 43 | NW | CFRP | 1506 | 120.0 | 1.10 | 51.0 | 32.6 | 1.57 |
| | C15N | R | 2.50 | 0.13 | 0.38 | 0.31 | 3.71 | 34 | NW | CFRP | 1506 | 120.0 | 1.54 | 57.9 | 36.0 | 1.61 |
| Deitz et al. (1999) | GFRP1 | R | 2.13 | 0.31 | 0.19 | 0.16 | 4.50 | 29 | NW | GFRP | 650 | 40.0 | 0.73 | 27.8 | 24.6 | 1.13 |
| | GFRP2 | R | 2.74 | 0.31 | 0.19 | 0.16 | 5.80 | 30 | NW | GFRP | 650 | 40.0 | 0.73 | 29.6 | 24.9 | 1.19 |
| | GFRP3 | R | 2.74 | 0.31 | 0.19 | 0.16 | 5.80 | 27 | NW | GFRP | 650 | 40.0 | 0.73 | 30.5 | 23.9 | 1.27 |
| Duranovic et al., (1997) | GB2 | R | 2.30 | 0.15 | 0.25 | 0.21 | 3.65 | 38 | NW | GFRP | 800 | 45.0 | 1.31 | 27.2 | 21.1 | 1.29 |
| | GB6 | R | 2.30 | 0.15 | 0.25 | 0.21 | 3.65 | 33 | NW | GFRP | 800 | 45.0 | 1.36 | 22.7 | 20.2 | 1.12 |
| Bentz et al. (2010) | L05-0 | R | 7.10 | 0.45 | 0.10 | 0.94 | 3.26 | 46 | NW | GFRP | 397 | 37.0 | 0.51 | 142.3 | 88.7 | 1.60 |
| | M05-0 | R | 3.05 | 0.45 | 0.50 | 0.44 | 3.48 | 35 | NW | GFRP | 474 | 37 | 0.55 | 87.80 | 77.2 | 1.14 |
| | S05-0 | R | 1.52 | 0.45 | 0.25 | 0.194 | 3.93 | 35 | NW | GFRP | 397 | 37 | 0.66 | 55.10 | 48.5 | 1.14 |
| | L20-0 | R | 7.10 | 0.45 | 0.10 | 0.857 | 3.56 | 36 | NW | GFRP | 397 | 37 | 2.23 | 240.30 | 155.1 | 1.55 |
| | M05-0 | R | 3.05 | 0.45 | 0.50 | 0.405 | 3.77 | 35 | NW | GFRP | 397 | 37 | 2.36 | 140.30 | 115.1 | 1.22 |
| | S20-0 | R | 1.52 | 0.45 | 0.25 | 0.188 | 4.05 | 35 | NW | GFRP | 397 | 37 | 2.54 | 74.60 | 68.8 | 1.08 |
| Kim and Jang (2014) | C-2.5-R1 | R | 2.20 | 0.20 | 0.25 | 0.22 | 2.5 | 30 | NW | CFRP | 2130 | 146.2 | 0.32 | 35.40 | 24.1 | 1.47 |
| | C-2.5-R2 | R | 2.20 | 0.15 | 0.25 | 0.22 | 2.5 | 30 | NW | CFRP | 2130.00 | 146.20 | 0.43 | 25 | 19.6 | 1.28 |
| | C-2.5-R3 | R | 2.20 | 0.15 | 0.25 | 0.22 | 2.50 | 30 | NW | CFRP | 2023 | 147.9 | 0.77 | 26.1 | 23.0 | 1.14 |
| | C-3.5-R1 | R | 2.20 | 0.20 | 0.25 | 0.22 | 3.50 | 30 | NW | CFRP | 2130 | 146.2 | 0.32 | 29.4 | 24.1 | 1.22 |
| | C-3.5-R2 | R | 2.20 | 0.15 | 0.25 | 0.22 | 3.50 | 30 | NW | CFRP | 2130 | 146.2 | 0.43 | 26.9 | 19.6 | 1.37 |

**Table 2** (continued)

| Authors | Specimen | Cross-section | $L$ (m) | $b_w$ (m) | $h$ (m) | $d$ (m) | $a/d$ | $f'_c$ (MPa) | Concrete type | FRP type | $f_{fu}$ (MPa) | $E_f$ (GPa) | $\rho_f$ (%) | $V_{c,test}$ (kN) | $V_{c,KDS}$ (kN) | $V_{c,test}/V_{c,KDS}$ |
|---|---|---|---|---|---|---|---|---|---|---|---|---|---|---|---|---|
| | C-3.5-R3 | R | 2.20 | 0.15 | 0.25 | 0.22 | 3.50 | 30 | NW | CFRP | 2023 | 147.9 | 0.77 | 29.6 | 23.0 | 1.29 |
| | C-4.5-R1 | R | 2.20 | 0.20 | 0.25 | 0.22 | 4.50 | 30 | NW | CFRP | 2130 | 146.2 | 0.32 | 26.6 | 24.1 | 1.10 |
| | C-4.5-R2 | R | 2.20 | 0.15 | 0.25 | 0.22 | 4.50 | 30 | NW | CFRP | 2130 | 146.2 | 0.43 | 24.6 | 19.6 | 1.26 |
| | C-4.5-R3 | R | 2.20 | 0.15 | 0.25 | 0.22 | 4.50 | 30 | NW | CFRP | 2023 | 147.9 | 0.77 | 28.1 | 23.0 | 1.22 |
| | G-2.5-R1 | R | 2.20 | 0.20 | 0.25 | 0.22 | 2.50 | 30 | NW | GFRP | 980 | 48.2 | 0.32 | 25.7 | 17.9 | 1.44 |
| | G-2.5-R2 | R | 2.20 | 0.15 | 0.25 | 0.22 | 2.50 | 30 | NW | GFRP | 980 | 48.2 | 0.43 | 24.4 | 14.5 | 1.68 |
| | G-2.5-R3 | R | 2.20 | 0.15 | 0.25 | 0.22 | 2.50 | 30 | NW | GFRP | 941 | 49.1 | 0.77 | 27.3 | 17.1 | 1.60 |
| | G-3.5-R1 | R | 2.20 | 0.20 | 0.25 | 0.22 | 3.50 | 30 | NW | GFRP | 980 | 48.2 | 0.32 | 27.2 | 17.9 | 1.52 |
| | G-3.5-R2 | R | 2.20 | 0.15 | 0.25 | 0.22 | 3.50 | 30 | NW | GFRP | 980 | 48.2 | 0.43 | 21.1 | 14.5 | 1.45 |
| | G-3.5-R3 | R | 2.20 | 0.15 | 0.25 | 0.22 | 3.50 | 30 | NW | GFRP | 941 | 49.1 | 0.77 | 19.5 | 17.1 | 1.14 |
| | G-4.5-R1 | R | 2.20 | 0.20 | 0.25 | 0.22 | 4.50 | 30 | NW | GFRP | 980 | 48.2 | 0.32 | 20.0 | 17.9 | 1.12 |
| | G-4.5-R2 | R | 2.20 | 0.15 | 0.25 | 0.22 | 4.50 | 30 | NW | GFRP | 980 | 48.2 | 0.43 | 17.2 | 14.5 | 1.18 |
| | G-4.5-R3 | R | 2.20 | 0.15 | 0.25 | 0.22 | 4.50 | 30 | NW | GFRP | 941 | 49.1 | 0.77 | 20.5 | 17.1 | 1.20 |
| | C-L-18-R1 | R | 2.00 | 0.20 | 0.25 | 0.22 | 3.00 | 34 | LW | CFRP | 2130 | 146.2 | 0.32 | 26.2 | 21.4 | 1.22 |
| | C-L-18-R2 | R | 2.00 | 0.15 | 0.25 | 0.22 | 3.00 | 34 | LW | CFRP | 2130 | 146.2 | 0.43 | 19.2 | 17.4 | 1.10 |
| | C-L-27-R1 | R | 2.00 | 0.20 | 0.25 | 0.22 | 3.00 | 40 | LW | CFRP | 2130 | 146.2 | 0.32 | 23.6 | 22.8 | 1.04 |
| | C-L-27-R2 | R | 2.00 | 0.15 | 0.25 | 0.22 | 3.00 | 40 | LW | CFRP | 2130 | 146.2 | 0.43 | 21.4 | 18.5 | 1.16 |
| | C-L-27-R3 | R | 2.00 | 0.15 | 0.25 | 0.22 | 3.00 | 40 | LW | CFRP | 2023 | 147.9 | 0.77 | 26.5 | 21.7 | 1.22 |
| | G-L-18-R1 | R | 2.00 | 0.20 | 0.25 | 0.22 | 3.00 | 34 | LW | GFRP | 980 | 48.2 | 0.32 | 21.1 | 15.9 | 1.32 |
| | G-L-18-R2 | R | 2.00 | 0.15 | 0.25 | 0.22 | 3.00 | 34 | LW | GFRP | 980 | 48.2 | 0.43 | 18.9 | 12.9 | 1.46 |
| | G-L-27-R1 | R | 2.00 | 0.20 | 0.25 | 0.22 | 3.00 | 40 | LW | GFRP | 980 | 48.2 | 0.32 | 20.8 | 16.9 | 1.23 |
| | G-L-27-R2 | R | 2.00 | 0.15 | 0.25 | 0.22 | 3.00 | 40 | LW | GFRP | 980 | 48.2 | 0.43 | 20.3 | 13.7 | 1.48 |
| | G-L-27-R3 | R | 2.00 | 0.15 | 0.25 | 0.22 | 3.00 | 40 | LW | GFRP | 941 | 49.1 | 0.77 | 21.8 | 16.1 | 1.35 |
| Guadagnini et al. (2006) | GB43 | R | 2.30 | 0.15 | 0.25 | 0.22 | 3.30 | 40 | NW | GFRP | 765 | 45.0 | 1.10 | 27.9 | 20.4 | 1.37 |
| Matta et al. (2013) | S1-0.12-1A | R | 7.32 | 0.46 | 0.98 | 0.88 | 3.10 | 30 | NW | GFRP | 476 | 41.0 | 0.60 | 179.6 | 128.4 | 1.40 |
| | S1-0.12-2B | R | 7.32 | 0.46 | 0.98 | 0.88 | 3.10 | 30 | NW | GFRP | 483 | 41.0 | 0.60 | 176.9 | 128.4 | 1.38 |
| | S3-0.12-1A | R | 2.13 | 0.11 | 0.33 | 0.29 | 3.10 | 32 | NW | GFRP | 849 | 43.2 | 0.60 | 19.8 | 14.8 | 1.34 |
| | S3-0.12-2A | R | 2.13 | 0.11 | 0.33 | 0.29 | 3.10 | 32 | NW | GFRP | 849 | 43.2 | 0.60 | 18.5 | 14.8 | 1.25 |
| | S6-0.12-1A | R | 1.22 | 0.23 | 0.18 | 0.15 | 3.10 | 60 | NW | GFRP | 849 | 43.2 | 0.60 | 29.0 | 21.9 | 1.33 |
| | S6-0.12-2A | R | 1.22 | 0.23 | 0.18 | 0.15 | 3.10 | 32 | NW | GFRP | 849 | 43.2 | 0.60 | 37.3 | 17.6 | 2.12 |
| | S6-0.12-3A | R | 1.22 | 0.23 | 0.18 | 0.15 | 3.10 | 32 | NW | GFRP | 849 | 43.2 | 0.60 | 26.7 | 17.3 | 1.54 |
| | S1-0.24-1A | R | 7.32 | 0.46 | 0.98 | 0.88 | 3.10 | 30 | NW | GFRP | 476 | 41.0 | 1.20 | 246.2 | 154.9 | 1.59 |
| | S1-0.24-2B | R | 7.32 | 0.46 | 0.98 | 0.88 | 3.10 | 31 | NW | GFRP | 483 | 41.0 | 1.20 | 238.2 | 156.8 | 1.52 |
| | S3-0.24-1B | R | 2.13 | 0.11 | 0.33 | 0.29 | 3.10 | 41 | NW | GFRP | 751 | 48.2 | 1.21 | 22.6 | 20.1 | 1.12 |
| | S3-0.24-2B | R | 2.13 | 0.11 | 0.33 | 0.29 | 3.10 | 41 | NW | GFRP | 751 | 48.2 | 1.21 | 21.2 | 20.1 | 1.05 |
| | S6-0.24-1B | R | 1.22 | 0.23 | 0.18 | 0.15 | 3.10 | 41 | NW | GFRP | 751 | 48.2 | 1.20 | 33.4 | 23.5 | 1.42 |

**Table 2** (continued)

| Authors | Specimen | Cross-section | $L$ (m) | $b_w$ (m) | $h$ (m) | $d$ (m) | $a/d$ | $f'_c$ (MPa) | Concrete type | FRP type | $f_{fu}$ (MPa) | $E_f$ (GPa) | $\rho_f$ (%) | $V_{c,test}$ (kN) | $V_{c,KDS}$ (kN) | $V_{c,test}/V_{c,KDS}$ |
|---|---|---|---|---|---|---|---|---|---|---|---|---|---|---|---|---|
| | S6-0.24-2B | R | 1.22 | 0.23 | 0.18 | 0.15 | 3.10 | 41 | NW | GFRP | 751 | 48.2 | 1.20 | 32.9 | 23.5 | 1.40 |
| Olivito and Zuccarello (2010) | Series I(5) | R | 2.00 | 0.15 | 0.20 | 0.18 | 5.60 | 20 | NW | CFRP | 1725 | 115.0 | 0.87 | 19.1 | 15.7 | 1.22 |
| | Series II(5) | R | 2.00 | 0.15 | 0.20 | 0.18 | 5.60 | 20 | NW | CFRP | 1725 | 115.0 | 1.46 | 24.4 | 19.8 | 1.23 |
| | Series III(5) | R | 2.00 | 0.15 | 0.20 | 0.18 | 5.60 | 27 | NW | CFRP | 1725 | 115.0 | 0.87 | 26.2 | 18.6 | 1.41 |
| | Series IV(5) | R | 2.00 | 0.15 | 0.20 | 0.18 | 5.60 | 27 | NW | CFRP | 1725 | 115.0 | 1.46 | 27.5 | 21.8 | 1.26 |
| Alam (2010) | G-2.5 | R | 2.40 | 0.25 | 0.35 | 0.31 | 2.50 | 39 | NW | GFRP | 751 | 48.0 | 0.84 | 62.8 | 41.1 | 1.53 |
| | G-3.5 | R | 3.10 | 0.25 | 0.35 | 0.31 | 3.50 | 39 | NW | GFRP | 751 | 48.0 | 0.84 | 45.9 | 41.1 | 1.12 |
| | C-2.5 | R | 2.40 | 0.25 | 0.35 | 0.31 | 2.50 | 33 | NW | CFRP | 1899 | 144.0 | 0.42 | 79.0 | 44.4 | 1.78 |
| | C-3.5 | R | 3.10 | 0.25 | 0.35 | 0.31 | 3.50 | 33 | NW | CFRP | 1899 | 144.0 | 0.42 | 61.1 | 43.0 | 1.42 |
| | G-500 | R | 3.10 | 0.25 | 0.50 | 0.44 | 2.50 | 43 | NW | GFRP | 751 | 48.0 | 0.89 | 132.5 | 58.8 | 2.25 |
| | G-650 | R | 3.60 | 0.30 | 0.65 | 0.58 | 2.50 | 36 | NW | GFRP | 751 | 48.0 | 0.91 | 118.1 | 77.5 | 1.52 |
| | G-500-70 | R | 3.10 | 0.25 | 0.50 | 0.44 | 2.50 | 72 | NW | GFRP | 751 | 48.2 | 1.46 | 119.2 | 77.8 | 1.53 |
| | G-650-70 | R | 3.60 | 0.30 | 0.65 | 0.58 | 2.50 | 72 | NW | GFRP | 751 | 48.2 | 1.51 | 160.5 | 114.7 | 1.40 |
| | C-500 | R | 3.10 | 0.25 | 0.50 | 0.46 | 2.50 | 41 | NW | CFRP | 1899 | 144.0 | 0.44 | 67.6 | 61.4 | 1.10 |
| | C-650 | R | 3.60 | 0.30 | 0.65 | 0.59 | 2.50 | 36 | NW | CFRP | 1899 | 144.0 | 0.43 | 143.7 | 85.0 | 1.69 |
| | C-500-70 | R | 3.10 | 0.25 | 0.50 | 0.45 | 2.50 | 72 | NW | CFRP | 1899 | 144.0 | 0.82 | 103.5 | 89.4 | 1.16 |
| | C-650-70 | R | 3.60 | 0.30 | 0.65 | 0.59 | 2.50 | 72 | NW | CFRP | 1899 | 144.0 | 0.73 | 151.3 | 126.4 | 1.20 |
| | G-2.5-350(1) | R | 2.40 | 0.25 | 0.35 | 0.30 | 2.50 | 36 | NW | GFRP | 786 | 46.3 | 1.41 | 67.3 | 45.5 | 1.48 |
| | G-2.5-350(2) | R | 2.40 | 0.25 | 0.35 | 0.30 | 2.50 | 36 | NW | GFRP | 786 | 46.3 | 1.41 | 72.7 | 45.5 | 1.60 |
| | G-0.5-500 | R | 3.10 | 0.25 | 0.50 | 0.46 | 2.50 | 41 | NW | GFRP | 786 | 46.3 | 0.35 | 71.1 | 42.5 | 1.67 |
| | G-2.5-500 | R | 3.10 | 0.25 | 0.50 | 0.43 | 2.50 | 41 | NW | GFRP | 786 | 46.3 | 1.46 | 95.3 | 62.8 | 1.52 |
| | C-0.5-350 | R | 2.40 | 0.25 | 0.35 | 0.31 | 2.50 | 41 | NW | CFRP | 1899 | 144.0 | 0.18 | 60.5 | 37.1 | 1.63 |
| | C-2.5-350 | R | 2.40 | 0.25 | 0.35 | 0.31 | 2.50 | 41 | NW | CFRP | 1899 | 144.0 | 0.66 | 74.3 | 52.6 | 1.41 |
| | C-0.5-500 | R | 3.10 | 0.25 | 0.50 | 0.46 | 2.50 | 41 | NW | CFRP | 1899 | 144.0 | 0.22 | 73.3 | 50.8 | 1.44 |
| | C-2.5-500 | R | 3.10 | 0.25 | 0.50 | 0.44 | 2.50 | 41 | NW | CFRP | 1899 | 144.0 | 0.65 | 85.6 | 68.5 | 1.25 |
| | G50 | R | 2.40 | 0.25 | 0.35 | 0.29 | 2.50 | 63 | NW | GFRP | 786 | 46.3 | 0.87 | 77.4 | 49.2 | 1.57 |
| | G-70 | R | 2.40 | 0.25 | 0.35 | 0.29 | 2.50 | 85 | NW | GFRP | 786 | 46.3 | 0.87 | 82.0 | 55.0 | 1.49 |
| | C50 | R | 2.40 | 0.25 | 0.35 | 0.31 | 2.50 | 63 | NW | CFRP | 1899 | 144.0 | 0.42 | 73.4 | 54.5 | 1.35 |
| Nakamura and Higai (1995) | G01 | R | 1.20 | 0.30 | 0.20 | 0.15 | 4.00 | 23 | NW | GFRP | 751 | 29.0 | 1.34 | 33.5 | 24.9 | 1.34 |
| | G02 | R | 1.20 | 0.30 | 0.20 | 0.15 | 4.00 | 28 | NW | GFRP | 751 | 29.0 | 1.79 | 36.5 | 28.9 | 1.26 |
| Swamy and Aburawi (1997) | F3-CF | R | 2.10 | 0.15 | 0.25 | 0.22 | 3.15 | 39 | NW | GFRP | 586 | 34.0 | 1.55 | 39.7 | 22.3 | 1.78 |
| Liu (2011) | #1 B1NW | R | 2.44 | 0.64 | 0.24 | 0.20 | 6.04 | 72 | NW | GFRP | 715 | 43.3 | 0.94 | 138.4 | 96.9 | 1.43 |
| | #2 B2NW | R | 2.44 | 0.64 | 0.24 | 0.20 | 6.04 | 87 | NW | GFRP | 715 | 43.3 | 0.94 | 136.6 | 103.8 | 1.32 |
| | #3 B2NW | R | 2.44 | 0.64 | 0.24 | 0.20 | 6.04 | 60 | NW | GFRP | 715 | 43.3 | 0.94 | 125.0 | 90.6 | 1.38 |
| | #4 B1LW | R | 2.44 | 0.64 | 0.24 | 0.20 | 6.04 | 63 | LW | GFRP | 715 | 43.3 | 0.94 | 113.9 | 78.4 | 1.45 |

**Table 2** (continued)

| Authors | Specimen | Cross-section | $L$ (m) | $b_w$ (m) | $h$ (m) | $d$ (m) | $a/d$ | $f'_c$ (MPa) | Concrete type | FRP type | $f_{fu}$ (MPa) | $E_f$ (GPa) | $\rho_f$ (%) | $V_{c,test}$ (kN) | $V_{c,KDS}$ (kN) | $V_{c,test}/V_{c,KDS}$ |
|---|---|---|---|---|---|---|---|---|---|---|---|---|---|---|---|---|
| | #5 B1LW | R | 2.44 | 0.64 | 0.24 | 0.20 | 6.04 | 75 | LW | GFRP | 715 | 43.3 | 0.94 | 104.1 | 83.6 | 1.25 |
| | #6 B2LW | R | 2.44 | 0.64 | 0.24 | 0.20 | 6.04 | 60 | LW | GFRP | 715 | 43.3 | 0.94 | 104.6 | 77.0 | 1.36 |
| | #7 B1LW | R | 2.03 | 0.64 | 0.26 | 0.23 | 4.47 | 68 | LW | GFRP | 715 | 43.3 | 0.94 | 124.0 | 87.1 | 1.42 |
| | #8 B1NW | R | 2.90 | 0.64 | 0.27 | 0.24 | 6.04 | 79 | NW | GFRP | 715 | 43.3 | 0.79 | 109.0 | 107.1 | 1.02 |
| | #9 B2NW | R | 2.90 | 0.64 | 0.27 | 0.24 | 6.04 | 61 | NW | GFRP | 715 | 43.3 | 0.79 | 126.4 | 97.4 | 1.30 |
| | #10 B1LW | R | 2.90 | 0.64 | 0.27 | 0.24 | 6.04 | 63 | LW | GFRP | 715 | 43.3 | 0.79 | 101.0 | 83.8 | 1.21 |
| | #11 B2LW | R | 2.90 | 0.64 | 0.27 | 0.24 | 6.04 | 67 | LW | GFRP | 715 | 43.3 | 0.79 | 106.8 | 85.7 | 1.25 |
| | #12 B1NW | R | 2.44 | 1.85 | 0.24 | 0.20 | 6.04 | 84 | NW | GFRP | 715 | 43.3 | 0.96 | 396.3 | 301.0 | 1.32 |
| | #13 B2NW | R | 2.44 | 1.85 | 0.24 | 0.20 | 6.04 | 59 | NW | GFRP | 715 | 43.3 | 0.96 | 330.0 | 264.4 | 1.25 |
| | #14 B1LW | R | 2.44 | 1.85 | 0.24 | 0.20 | 6.04 | 63 | LW | GFRP | 715 | 43.3 | 0.96 | 279.3 | 230.2 | 1.21 |
| | #15 B1LW | R | 2.44 | 1.85 | 0.24 | 0.20 | 6.04 | 63 | LW | GFRP | 715 | 43.3 | 0.96 | 294.9 | 230.2 | 1.28 |
| | #16 B2LW | R | 2.44 | 1.85 | 0.24 | 0.20 | 6.04 | 57 | LW | GFRP | 715 | 43.3 | 0.96 | 303.8 | 222.0 | 1.37 |
| | #17 B2LW | R | 2.44 | 1.85 | 0.24 | 0.20 | 6.04 | 56 | LW | GFRP | 715 | 43.3 | 0.96 | 307.3 | 220.5 | 1.39 |
| | #18 B1NWE | R | 2.44 | 1.85 | 0.24 | 0.20 | 6.04 | 84 | NW | GFRP | 715 | 43.3 | 0.54 | 282.9 | 258.4 | 1.09 |
| | #19 B1LWE | R | 2.44 | 1.85 | 0.24 | 0.20 | 6.04 | 63 | LW | GFRP | 715 | 43.3 | 0.54 | 254.0 | 197.6 | 1.29 |
| | #20 B2LWE | R | 2.44 | 1.85 | 0.24 | 0.20 | 6.04 | 56 | LW | GFRP | 715 | 43.3 | 0.54 | 225.9 | 189.2 | 1.19 |
| Razaqpur et al. (2011) | B1 | R | 3.00 | 0.30 | 0.23 | 0.20 | 3.50 | 52 | NW | CFRP | 1500 | 114.0 | 0.35 | 64.6 | 39.6 | 1.63 |
| | B2 | R | 3.00 | 0.30 | 0.33 | 0.30 | 3.50 | 52 | NW | CFRP | 1500 | 114.0 | 0.32 | 62.3 | 50.7 | 1.23 |
| | B3 | R | 3.00 | 0.30 | 0.43 | 0.40 | 3.50 | 52 | NW | CFRP | 1500 | 114.0 | 0.30 | 57.3 | 60.6 | 0.95 |
| | B4 | R | 3.00 | 0.30 | 0.53 | 0.50 | 3.50 | 52 | NW | CFRP | 1500 | 114.0 | 0.28 | 71.5 | 69.4 | 1.03 |
| | B5 | R | 3.00 | 0.30 | 0.43 | 0.40 | 6.50 | 52 | NW | CFRP | 1500 | 114.0 | 0.30 | 55.2 | 60.6 | 0.91 |
| | B6 | R | 3.00 | 0.30 | 0.43 | 0.40 | 6.00 | 52 | NW | CFRP | 1500 | 114.0 | 0.30 | 65.9 | 60.6 | 1.09 |
| Zeidan et al (2011) | A-II-2.5 | R | 2.00 | 0.15 | 0.30 | 0.28 | 2.50 | 45 | NW | CFRP | 2840 | 148.0 | 0.11 | 23.2 | 18.0 | 1.29 |
| | A-II-5.0 | R | 3.40 | 0.15 | 0.30 | 0.28 | 5.00 | 49 | NW | CFRP | 2840 | 148.0 | 0.11 | 13.6 | 18.5 | 0.73 |
| | B-II-2.5 | R | 2.00 | 0.15 | 0.30 | 0.28 | 2.50 | 46 | NW | CFRP | 2840 | 148.0 | 0.21 | 28.2 | 21.5 | 1.31 |
| | A-I-2.5 | R | 2.00 | 0.15 | 0.30 | 0.28 | 2.50 | 24 | NW | CFRP | 2840 | 148.0 | 0.11 | 23.2 | 14.3 | 1.63 |
| Khaja and Sherwood (2013) | MB-1 | R | 1.50 | 0.40 | 0.28 | 0.25 | 3.00 | 51 | NW | GFRP | 728 | 47.5 | 0.57 | 57.1 | 54.9 | 1.04 |
| | MB-2 | R | 1.50 | 0.40 | 0.28 | 0.25 | 3.00 | 49 | NW | GFRP | 728 | 47.5 | 0.86 | 75.1 | 60.4 | 1.24 |
| | MB-3 | R | 1.50 | 0.40 | 0.28 | 0.25 | 3.00 | 51 | NW | GFRP | 728 | 47.5 | 1.14 | 86.1 | 66.2 | 1.30 |
| | MB-4 | R | 1.50 | 0.40 | 0.28 | 0.25 | 3.00 | 51 | NW | GFRP | 728 | 47.5 | 1.71 | 109.1 | 73.8 | 1.48 |
| | MB-5 | R | 1.50 | 0.40 | 0.28 | 0.25 | 3.00 | 52 | NW | GFRP | 728 | 47.5 | 2.28 | 116.1 | 80.4 | 1.44 |
| | MB-6 | R | 1.50 | 0.40 | 0.28 | 0.25 | 3.00 | 50 | NW | GFRP | 728 | 47.5 | 0.86 | 79.1 | 60.9 | 1.30 |
| | MB-7 | R | 2.00 | 0.40 | 0.28 | 0.25 | 4.00 | 51 | NW | GFRP | 728 | 47.5 | 1.14 | 90.4 | 66.2 | 1.37 |
| | MB-8 | R | 3.00 | 0.40 | 0.28 | 0.25 | 6.00 | 50 | NW | GFRP | 728 | 47.5 | 1.71 | 91.1 | 73.3 | 1.24 |
| | MB-9 | R | 4.00 | 0.40 | 0.28 | 0.25 | 8.00 | 48 | NW | GFRP | 728 | 47.5 | 2.28 | 84.8 | 78.1 | 1.09 |
| | MB-10 | R | 1.50 | 0.40 | 0.28 | 0.25 | 3.00 | 51 | NW | GFRP | 675 | 51.9 | 4.05 | 136.1 | 101.9 | 1.34 |

**Table 2** (continued)

| Authors | Specimen | Cross-section | $L$ (m) | $b_w$ (m) | $h$ (m) | $d$ (m) | $a/d$ | $f'_c$ (MPa) | Concrete type | FRP type | $f_{fu}$ (MPa) | $E_f$ (GPa) | $\rho_f$ (%) | $V_{c,test}$ (kN) | $V_{c,KDS}$ (kN) | $V_{c,test}/V_{c,KDS}$ |
|---|---|---|---|---|---|---|---|---|---|---|---|---|---|---|---|---|
| | MB-11 | R | 4.00 | 0.40 | 0.28 | 0.25 | 8.00 | 48 | NW | GFRP | 675 | 51.9 | 4.05 | 99.8 | 93.4 | 1.07 |
| Farahmand (1996) | Beam #1 | R | 2.00 | 0.20 | 0.30 | 0.25 | 4.00 | 31 | NW | GFRP | 692 | 41.3 | 0.68 | 24.5 | 24.6 | 1.00 |
| | Beam #2 | R | 2.00 | 0.20 | 0.30 | 0.25 | 4.00 | 31 | NW | GFRP | 692 | 41.3 | 0.79 | 26.6 | 25.6 | 1.04 |
| | Beam #3 | R | 2.00 | 0.20 | 0.30 | 0.25 | 4.00 | 31 | NW | GFRP | 692 | 41.3 | 1.08 | 33.4 | 27.8 | 1.20 |
| | Beam #4 | R | 1.50 | 0.20 | 0.30 | 0.25 | 3.00 | 35 | NW | GFRP | 692 | 41.3 | 0.51 | 30.5 | 23.8 | 1.28 |
| | Beam #5 | R | 1.50 | 0.20 | 0.30 | 0.25 | 3.00 | 35 | NW | GFRP | 692 | 41.3 | 0.76 | 39.9 | 26.5 | 1.51 |
| | Beam #6 | R | 1.50 | 0.20 | 0.30 | 0.25 | 3.00 | 35 | NW | GFRP | 692 | 41.3 | 1.01 | 37.8 | 28.5 | 1.32 |
| Ashour and Kara (2014) | B-400-2 | R | 2.80 | 0.20 | 0.40 | 0.37 | 2.70 | 22 | NW | CFRP | 1100 | 141.0 | 0.12 | 34.7 | 23.1 | 1.50 |
| | B-400-4 | R | 2.80 | 0.20 | 0.40 | 0.37 | 2.70 | 22 | NW | CFRP | 1100 | 141.0 | 0.24 | 37.9 | 27.9 | 1.36 |
| | B-300-2 | R | 2.80 | 0.20 | 0.30 | 0.27 | 3.60 | 29 | NW | CFRP | 1100 | 141.0 | 0.16 | 34.2 | 22.4 | 1.53 |
| | B-300-4 | R | 2.80 | 0.20 | 0.30 | 0.27 | 3.60 | 29 | NW | CFRP | 1100 | 141.0 | 0.33 | 34.2 | 27.2 | 1.26 |
| | B-200-2 | R | 2.80 | 0.20 | 0.20 | 0.17 | 5.90 | 24 | NW | CFRP | 1100 | 141.0 | 0.26 | 18.5 | 16.9 | 1.10 |
| | B-200-4 | R | 2.80 | 0.20 | 0.20 | 0.17 | 5.90 | 24 | NW | CFRP | 1100 | 141.0 | 0.52 | 21.7 | 20.3 | 1.07 |
| Abdul-Salam (2014) | GA-56 | R | 3.49 | 1.00 | 0.20 | 0.14 | 6.07 | 48 | NW | GFRP | 724 | 41.0 | 1.01 | 100.6 | 110.2 | 0.91 |
| | GV-46 | R | 3.49 | 1.00 | 0.20 | 0.14 | 6.07 | 48 | NW | GFRP | 588 | 47.6 | 0.79 | 125.1 | 107.5 | 1.16 |
| | GV-56 | R | 3.49 | 1.00 | 0.20 | 0.14 | 6.07 | 48 | NW | GFRP | 588 | 47.6 | 1.01 | 112.1 | 114.5 | 0.98 |
| | GV-66 | R | 3.49 | 1.00 | 0.20 | 0.14 | 6.07 | 48 | NW | GFRP | 588 | 47.6 | 1.22 | 125.1 | 120.3 | 1.04 |
| | GV-76 | R | 3.49 | 1.00 | 0.20 | 0.14 | 6.07 | 50 | NW | GFRP | 588 | 47.6 | 1.42 | 170.0 | 127.1 | 1.34 |
| | GV-58 | R | 3.49 | 1.00 | 0.20 | 0.14 | 6.18 | 48 | NW | GFRP | 666 | 51.9 | 1.85 | 151.8 | 136.8 | 1.11 |
| | GH-56 | R | 3.49 | 1.00 | 0.20 | 0.14 | 6.07 | 43 | NW | GFRP | 1197 | 69.5 | 1.01 | 174.6 | 121.4 | 1.44 |
| | GH-66 | R | 3.49 | 1.00 | 0.20 | 0.14 | 6.07 | 49 | NW | GFRP | 1197 | 69.5 | 1.21 | 128.1 | 133.5 | 0.96 |
| | GH-66B | R | 3.49 | 1.00 | 0.20 | 0.14 | 6.07 | 49 | NW | GFRP | 1197 | 69.5 | 2.43 | 126.6 | 159.9 | 0.79 |
| | GH-78 | R | 3.49 | 1.00 | 0.20 | 0.14 | 6.18 | 50 | NW | GFRP | 1197 | 69.5 | 2.55 | 127.6 | 162.7 | 0.78 |
| | GH-56a | R | 3.49 | 1.00 | 0.20 | 0.14 | 6.07 | 77 | NW | GFRP | 1197 | 69.5 | 1.01 | 161.3 | 150.5 | 1.07 |
| | GH-56b | R | 3.49 | 1.00 | 0.20 | 0.14 | 6.07 | 83 | NW | GFRP | 1197 | 69.5 | 1.03 | 143.7 | 155.6 | 0.92 |
| | CV-54 | R | 3.49 | 1.00 | 0.20 | 0.14 | 5.92 | 50 | NW | CFRP | 1690 | 144.0 | 0.45 | 173.9 | 126.0 | 1.38 |
| | CV-64 | R | 3.49 | 1.00 | 0.20 | 0.14 | 5.92 | 50 | NW | CFRP | 1690 | 144.0 | 0.54 | 147.6 | 132.1 | 1.12 |
| | CV-74 | R | 3.49 | 1.00 | 0.20 | 0.14 | 5.92 | 52 | NW | CFRP | 1690 | 144.0 | 0.63 | 165.6 | 139.5 | 1.19 |
| | CV-84 | R | 3.49 | 1.00 | 0.20 | 0.14 | 5.92 | 45 | NW | CFRP | 1690 | 144.0 | 0.72 | 163.6 | 137.0 | 1.19 |
| | CV-65 | R | 3.49 | 1.00 | 0.20 | 0.14 | 5.96 | 46 | NW | CFRP | 1690 | 140.0 | 0.84 | 179.6 | 142.7 | 1.26 |
| | CV-75 | R | 3.49 | 1.00 | 0.20 | 0.14 | 5.96 | 49 | NW | CFRP | 1690 | 140.0 | 0.98 | 192.6 | 152.0 | 1.27 |
| | CV-85 | R | 3.49 | 1.00 | 0.20 | 0.14 | 5.96 | 41 | NW | CFRP | 1690 | 140.0 | 1.11 | 198.6 | 147.0 | 1.35 |
| | CV-74a | R | 3.49 | 1.00 | 0.20 | 0.14 | 5.92 | 76 | NW | CFRP | 1690 | 144.0 | 0.63 | 174.6 | 160.6 | 1.09 |
| | CV-74b | R | 3.49 | 1.00 | 0.20 | 0.14 | 5.92 | 86 | NW | CFRP | 1690 | 144.0 | 0.63 | 219.4 | 168.1 | 1.31 |
| Gross et al. (2003) | FRP-1-26-HS | R | 2.13 | 0.20 | 0.29 | 0.23 | 4.06 | 80 | NW | GFRP | 690 | 40.3 | 1.25 | 38.9 | 40.1 | 0.97 |
| | FRP-2-26-HS | R | 2.13 | 0.15 | 0.29 | 0.23 | 4.06 | 80 | NW | GFRP | 690 | 40.3 | 1.66 | 33.2 | 32.4 | 1.03 |

**Table 2** (continued)

| Authors | Specimen | Cross-section | $L$ (m) | $b_w$ (m) | $h$ (m) | $d$ (m) | $a/d$ | $f'_c$ (MPa) | Concrete type | FRP type | $f_{fu}$ (MPa) | $E_f$ (GPa) | $\rho_f$ (%) | $V_{c,test}$ (kN) | $V_{c,KDS}$ (kN) | $V_{c,test}/V_{c,KDS}$ |
|---|---|---|---|---|---|---|---|---|---|---|---|---|---|---|---|---|
| | FRP-3-27-HS | R | 2.13 | 0.17 | 0.29 | 0.23 | 4.06 | 80 | NW | GFRP | 690 | 40.3 | 2.10 | 36.5 | 37.4 | 0.98 |
| | FRP-4-37-HS | R | 2.13 | 0.20 | 0.29 | 0.22 | 4.06 | 80 | NW | GFRP | 690 | 40.3 | 2.56 | 47.3 | 48.5 | 0.97 |
| Gross et al. (2004) | 8-2 | R | 1.97 | 0.13 | 0.17 | 0.14 | 6.36 | 60 | NW | CFRP | 2640 | 139.0 | 0.33 | 14.3 | 13.6 | 1.05 |
| | 8-3 | R | 1.97 | 0.16 | 0.17 | 0.14 | 6.45 | 62 | NW | CFRP | 2640 | 139.0 | 0.58 | 20.3 | 20.1 | 1.01 |
| | 11-2 | R | 1.97 | 0.09 | 0.17 | 0.14 | 6.36 | 81 | NW | CFRP | 2640 | 139.0 | 0.47 | 10.0 | 11.7 | 0.85 |
| | 11-3 | R | 1.97 | 0.12 | 0.17 | 0.14 | 6.45 | 81 | NW | CFRP | 2640 | 139.0 | 0.76 | 15.7 | 18.1 | 0.87 |
| Maruyama and Zhao (1994) | FN1 | R | 3.00 | 0.15 | 0.30 | 0.25 | 3.00 | 28 | NW | CFRP | 1308 | 94.0 | 0.55 | 38.3 | 21.2 | 1.80 |
| | FN2 | R | 3.00 | 0.15 | 0.30 | 0.25 | 3.00 | 33 | NW | CFRP | 1308 | 94.0 | 1.10 | 43.8 | 27.7 | 1.58 |
| | FN3 | R | 3.00 | 0.15 | 0.30 | 0.25 | 3.00 | 31 | NW | CFRP | 1308 | 94.0 | 1.39 | 48.3 | 30.4 | 1.59 |
| | FN4 | R | 3.00 | 0.15 | 0.30 | 0.25 | 3.00 | 35 | NW | CFRP | 1308 | 94.0 | 2.20 | 59.1 | 38.0 | 1.55 |
| Maruyama (1996) | #24 | R | 1.25 | 0.15 | 0.30 | 0.25 | 2.50 | 34 | NW | CFRP | 1200 | 100.0 | 1.04 | 38.8 | 27.0 | 1.43 |
| | #30 | R | 2.50 | 0.30 | 0.55 | 0.50 | 2.50 | 30 | NW | CFRP | 1200 | 100.0 | 1.04 | 145.4 | 85.1 | 1.71 |
| Caporale and Luciano (2009) | I | R | 2.00 | 0.15 | 0.20 | 0.17 | 4.12 | 24 | NW | GFRP | 1000 | 45.8 | 0.92 | 12.7 | 13.1 | 0.97 |
| | II | R | 2.00 | 0.15 | 0.20 | 0.17 | 4.12 | 24 | NW | GFRP | 1000 | 45.8 | 1.54 | 13.6 | 15.1 | 0.90 |
| | III | R | 2.00 | 0.15 | 0.20 | 0.17 | 4.12 | 31 | NW | GFRP | 1000 | 45.8 | 0.92 | 14.1 | 14.4 | 0.98 |
| | IV | R | 2.00 | 0.15 | 0.20 | 0.17 | 4.12 | 31 | NW | GFRP | 1000 | 45.8 | 1.54 | 15.3 | 16.6 | 0.92 |
| Niewels (2008) | Q-C-2L | R | 3.96 | 0.30 | 0.55 | 0.44 | 3.02 | 42 | NW | GFRP | 1000 | 62.6 | 3.65 | 145.4 | 112.9 | 1.29 |
| | Q-A-3L | R | 3.90 | 0.30 | 0.50 | 0.41 | 3.16 | 43 | NW | GFRP | 480 | 44.0 | 3.25 | 153.9 | 94.2 | 1.63 |
| | Q-A-5L | R | 4.50 | 0.30 | 0.50 | 0.40 | 3.71 | 28 | NW | GFRP | 1000 | 62.6 | 3.98 | 107.6 | 93.1 | 1.16 |
| Kilpatrick and Easden (2005) | 1a | R | 1.10 | 0.42 | 0.10 | 0.08 | 3.61 | 61 | NW | GFRP | 780 | 42.0 | 0.61 | 19.9 | 22.6 | 0.88 |
| | 1b | R | 1.50 | 0.42 | 0.10 | 0.08 | 6.10 | 61 | NW | GFRP | 725 | 42.0 | 1.10 | 25.5 | 26.4 | 0.97 |
| | 1c | R | 1.50 | 0.42 | 0.10 | 0.08 | 6.25 | 61 | NW | GFRP | 655 | 40.0 | 1.77 | 32.0 | 29.5 | 1.09 |
| | 1d | R | 1.50 | 0.42 | 0.10 | 0.08 | 6.41 | 61 | NW | GFRP | 630 | 40.0 | 2.61 | 40.5 | 32.6 | 1.24 |
| | 2a | R | 1.10 | 0.42 | 0.10 | 0.08 | 3.61 | 74 | NW | GFRP | 780 | 42.0 | 0.61 | 24.9 | 24.3 | 1.03 |
| | 2b | R | 1.50 | 0.42 | 0.10 | 0.08 | 6.10 | 74 | NW | GFRP | 725 | 42.0 | 1.10 | 22.0 | 28.3 | 0.78 |
| | 2c | R | 1.50 | 0.42 | 0.10 | 0.08 | 6.25 | 74 | NW | GFRP | 655 | 40.0 | 1.77 | 32.0 | 31.7 | 1.01 |
| | 2d | R | 1.50 | 0.42 | 0.10 | 0.08 | 6.41 | 74 | NW | GFRP | 630 | 40.0 | 2.61 | 36.5 | 35.0 | 1.04 |
| | 3a | R | 1.10 | 0.42 | 0.10 | 0.08 | 3.61 | 93 | NW | GFRP | 780 | 42.0 | 0.61 | 35.9 | 26.4 | 1.36 |
| | 3b | R | 1.50 | 0.42 | 0.10 | 0.08 | 6.10 | 93 | NW | GFRP | 725 | 42.0 | 1.10 | 23.0 | 30.8 | 0.75 |
| | 3c | R | 1.50 | 0.42 | 0.10 | 0.08 | 6.25 | 93 | NW | GFRP | 655 | 40.0 | 1.77 | 32.0 | 34.4 | 0.93 |
| | 3d | R | 1.50 | 0.42 | 0.10 | 0.08 | 6.41 | 93 | NW | GFRP | 630 | 40.0 | 2.61 | 38.5 | 38.0 | 1.01 |
| Kilpatrick and Dawborn (2006) | B1 | R | 0.90 | 0.42 | 0.10 | 0.08 | 6.00 | 48 | NW | GFRP | 840 | 42.0 | 0.68 | 24.8 | 21.1 | 1.17 |
| | B2 | R | 1.40 | 0.42 | 0.10 | 0.07 | 6.16 | 48 | NW | GFRP | 840 | 42.0 | 0.93 | 27.6 | 22.9 | 1.21 |
| | B3 | R | 0.90 | 0.42 | 0.10 | 0.07 | 6.16 | 48 | NW | GFRP | 840 | 42.0 | 1.16 | 29.6 | 24.2 | 1.22 |

**Table 2** (continued)

| Authors | Specimen | Cross-section | $L$ (m) | $b_w$ (m) | $h$ (m) | $d$ (m) | $a/d$ | $f'_c$ (MPa) | Concrete type | FRP type | $f_{fu}$ (MPa) | $E_f$ (GPa) | $\rho_f$ (%) | $V_{c,test}$ (kN) | $V_{c,KDS}$ (kN) | $V_{c,test}/V_{c,KDS}$ |
|---|---|---|---|---|---|---|---|---|---|---|---|---|---|---|---|---|
| | B4 | R | 0.90 | 0.42 | 0.10 | 0.08 | 6.00 | 76 | NW | GFRP | 840 | 42.0 | 0.68 | 27.5 | 25.0 | 1.10 |
| | B5 | R | 1.40 | 0.42 | 0.10 | 0.07 | 6.16 | 76 | NW | GFRP | 840 | 42.0 | 0.93 | 26.5 | 27.1 | 0.98 |
| | B6 | R | 0.90 | 0.42 | 0.10 | 0.07 | 6.16 | 76 | NW | GFRP | 840 | 42.0 | 1.16 | 31.4 | 28.7 | 1.09 |
| | B7 | R | 0.90 | 0.42 | 0.10 | 0.08 | 6.00 | 92 | NW | GFRP | 840 | 42.0 | 0.68 | 23.7 | 26.9 | 0.88 |
| | B8 | R | 1.40 | 0.42 | 0.10 | 0.07 | 6.16 | 92 | NW | GFRP | 840 | 42.0 | 0.93 | 25.7 | 29.1 | 0.88 |
| | B9 | R | 0.90 | 0.42 | 0.10 | 0.07 | 6.16 | 92 | NW | GFRP | 840 | 42.0 | 1.16 | 34.5 | 30.8 | 1.12 |
| Tomlinson and Fam (2015) | NT | R | 2.90 | 0.15 | 0.30 | 0.27 | 4.07 | 60 | NW | BFRP | 1100 | 70.0 | 0.39 | 19.8 | 23.0 | 0.86 |
| | NB | R | 2.90 | 0.15 | 0.30 | 0.27 | 4.07 | 60 | NW | BFRP | 1100 | 70.0 | 0.51 | 23.0 | 24.8 | 0.93 |
| | NC | R | 2.90 | 0.15 | 0.30 | 0.25 | 4.49 | 57 | NW | BFRP | 1100 | 70.0 | 0.85 | 28.6 | 28.2 | 1.01 |
| Krall (2014) | BM25-INF | R | 1.35 | 0.20 | 0.33 | 0.27 | 2.50 | 47 | NW | GFRP | 1000 | 64.0 | 1.82 | 82.1 | 47.8 | 1.72 |
| | BM16-INF | R | 1.35 | 0.20 | 0.35 | 0.27 | 2.50 | 47 | NW | GFRP | 1000 | 64.0 | 2.23 | 75.7 | 49.3 | 1.53 |
| | BM12-INF | R | 1.35 | 0.20 | 0.35 | 0.27 | 2.50 | 47 | NW | GFRP | 1000 | 64.0 | 2.51 | 63.1 | 51.5 | 1.23 |
| Johnson (2014) | JSC32-NT | R | 3.36 | 0.40 | 0.65 | 0.58 | 2.92 | 32 | NW | GFRP | 1265 | 61.2 | 1.00 | 159.5 | 108.6 | 1.47 |
| | JSV40-NT | R | 3.36 | 0.40 | 0.65 | 0.58 | 2.92 | 40 | NW | GFRP | 1264 | 71.2 | 1.00 | 169.0 | 122.7 | 1.38 |
| | JSC100-NT | R | 3.36 | 0.40 | 0.65 | 0.58 | 2.92 | 102 | NW | GFRP | 1265 | 61.2 | 1.00 | 166.0 | 165.8 | 1.00 |
| Noël and Soudki (2014) | G1 | R | 4.50 | 0.60 | 0.30 | 0.26 | 6.68 | 58 | NW | GFRP | 934 | 55.4 | 0.76 | 89.2 | 102.6 | 0.87 |
| | G2 | R | 4.50 | 0.60 | 0.30 | 0.26 | 6.68 | 58 | NW | GFRP | 934 | 55.4 | 1.51 | 116.2 | 123.5 | 0.94 |
| Chang and Seo (2012) | FS200-12 | R | 3.60 | 1.20 | 0.20 | 0.18 | 5.80 | 33 | NW | GFRP | 705 | 44 | 0.66 | 140.7 | 107.5 | 1.31 |
| | FS200-16 | R | 3.60 | 1.20 | 0.20 | 0.18 | 5.80 | 33 | NW | GFRP | 705 | 44 | 0.88 | 151.7 | 116.2 | 1.31 |
| | FS200-20 | R | 3.60 | 1.20 | 0.20 | 0.18 | 5.80 | 33 | NW | GFRP | 705 | 44 | 1.10 | 158.7 | 123.5 | 1.29 |
| | NFS200-6 | R | 3.60 | 1.20 | 0.20 | 0.18 | 5.80 | 33 | NW | GFRP | 1050 | 50 | 0.33 | 102.8 | 92.4 | 1.11 |
| | NFS200-8 | R | 3.60 | 1.20 | 0.20 | 0.18 | 5.80 | 33 | NW | GFRP | 1050 | 50 | 0.44 | 133.1 | 99.8 | 1.33 |
| | NFS200-12 | R | 3.60 | 1.20 | 0.20 | 0.18 | 5.80 | 33 | NW | GFRP | 1050 | 50 | 0.57 | 166.6 | 107.0 | 1.56 |
| El Refai and Abed (2016) | B-3.3-R1 | R | 1.60 | 0.15 | 0.25 | 0.22 | 3.30 | 49 | NW | BFRP | 1168 | 50 | 0.30 | 17.4 | 16.4 | 1.06 |
| | B-3.3-R2 | R | 1.60 | 0.15 | 0.25 | 0.22 | 3.30 | 49 | NW | BFRP | 1168 | 50 | 0.47 | 23.5 | 18.5 | 1.27 |
| | B-3.3-R3 | R | 1.60 | 0.15 | 0.25 | 0.22 | 3.30 | 49 | NW | BFRP | 1168 | 50 | 0.68 | 19.0 | 20.4 | 0.93 |
| | B-3.3-R4 | R | 1.60 | 0.15 | 0.25 | 0.22 | 3.30 | 49 | NW | BFRP | 1168 | 50 | 0.94 | 28.4 | 22.2 | 1.28 |
| | B-3.3-R5 | R | 1.60 | 0.15 | 0.25 | 0.22 | 3.30 | 49 | NW | BFRP | 1168 | 50 | 1.35 | 30.4 | 24.5 | 1.24 |
| | B-2.5-R1 | R | 1.60 | 0.15 | 0.25 | 0.22 | 2.50 | 49 | NW | BFRP | 1168 | 50 | 0.30 | 20.0 | 16.4 | 1.22 |
| | B-2.5-R2 | R | 1.60 | 0.15 | 0.25 | 0.22 | 2.50 | 49 | NW | BFRP | 1168 | 50 | 0.47 | 32.1 | 18.5 | 1.74 |
| | B-2.5-R3 | R | 1.60 | 0.15 | 0.25 | 0.22 | 2.50 | 49 | NW | BFRP | 1168 | 50 | 0.68 | 27.5 | 20.4 | 1.35 |
| Issa et al. (2016) | 5-10N5 | R | 3.05 | 0.20 | 0.30 | 0.17 | 5.56 | 36 | NW | BFRP | 1070 | 53 | 1.21 | 30.9 | 32.7 | 0.94 |
| | 5-13N5 | R | 3.05 | 0.20 | 0.30 | 0.17 | 5.56 | 36 | NW | BFRP | 1050 | 51 | 2.00 | 40.3 | 36.8 | 1.10 |
| | 5-16N5 | R | 3.05 | 0.20 | 0.30 | 0.17 | 5.56 | 36 | NW | BFRP | 1060 | 51 | 3.09 | 46.8 | 41.0 | 1.14 |
| | 6-16N7 | R | 3.05 | 0.20 | 0.30 | 0.17 | 7.00 | 36 | NW | BFRP | 1060 | 51 | 3.74 | 41.6 | 43.0 | 0.97 |
| | 3-25N7 | R | 3.05 | 0.20 | 0.30 | 0.17 | 7.00 | 36 | NW | BFRP | 1060 | 48 | 4.64 | 49.8 | 44.5 | 1.12 |

**Table 2** (continued)

| Authors | Specimen | Cross-section | $L$ (m) | $b_w$ (m) | $h$ (m) | $d$ (m) | $a/d$ | $f'_c$ (MPa) | Concrete type | FRP type | $f_{fu}$ (MPa) | $E_f$ (GPa) | $\rho_f$ (%) | $V_{c,test}$ (kN) | $V_{c,KDS}$ (kN) | $V_{c,test}/V_{c,KDS}$ |
|---|---|---|---|---|---|---|---|---|---|---|---|---|---|---|---|---|
| | 4-25N7 | R | 3.05 | 0.20 | 0.30 | 0.17 | 7.00 | 36 | NW | BFRP | 1060 | 48 | 6.18 | 52.9 | 47.7 | 1.11 |
| Acciai et al. (2016) | D-G1×13 | R | 2.00 | 0.10 | 0.20 | 0.18 | 5.56 | 41 | NW | GFRP | 690 | 40.8 | 0.74 | 10.2 | 9.8 | 1.04 |
| | D-G2×13 | R | 2.00 | 0.10 | 0.20 | 0.18 | 5.56 | 41 | NW | GFRP | 690 | 40.8 | 1.48 | 12.3 | 11.8 | 1.04 |
| | D-C1×9 | R | 2.00 | 0.10 | 0.20 | 0.18 | 5.56 | 66 | NW | CFRP | 2068 | 124 | 0.35 | 9.1 | 12.9 | 0.71 |
| | D-C2×9 | R | 2.00 | 0.10 | 0.20 | 0.18 | 5.56 | 66 | NW | CFRP | 2068 | 124 | 0.71 | 14.2 | 15.6 | 0.91 |
| Kaszubska et al. (2018) | G-512-30-15 | T | 1.80 | 0.15 | 0.40 | 0.38 | 2.90 | 31 | NW | GFRP | 1281 | 51.5 | 0.99 | 35.3 | 26.4 | 1.33 |
| | G-316-30-15 | T | 1.80 | 0.15 | 0.40 | 0.38 | 2.92 | 33 | NW | GFRP | 1205 | 51.5 | 1.07 | 32.8 | 27.7 | 1.19 |
| | G-318-30-15 | T | 1.80 | 0.15 | 0.40 | 0.38 | 2.93 | 33 | NW | GFRP | 1109 | 51.5 | 1.35 | 39.6 | 29.5 | 1.34 |
| | G-416-30-15 | T | 1.80 | 0.15 | 0.40 | 0.38 | 2.92 | 31 | NW | GFRP | 1205 | 51.5 | 1.42 | 35.8 | 29.2 | 1.23 |
| | G-418-30-15 | T | 1.80 | 0.15 | 0.40 | 0.38 | 2.93 | 33 | NW | GFRP | 1109 | 51.5 | 1.80 | 39.2 | 31.9 | 1.23 |
| | G-312/212–30-15 | T | 1.80 | 0.15 | 0.40 | 0.37 | 2.99 | 31 | NW | GFRP | 1281 | 51.5 | 1.02 | 35.8 | 26.7 | 1.34 |
| | G-318/118–30-15 | T | 1.80 | 0.15 | 0.40 | 0.37 | 3.00 | 33 | NW | GFRP | 1109 | 51.5 | 1.85 | 48.8 | 32.3 | 1.51 |
| Kurth (2012) | S1AN-0-1 | I | 6.00 | 0.10 | 0.65 | 0.57 | 3.53 | 34 | NW | GFRP | 1124 | 59 | 8.52 | 131.8 | 68.3 | 1.93 |
| | S3AH-0-5 | I | 6.00 | 0.10 | 0.65 | 0.57 | 3.53 | 80 | NW | GFRP | 1124 | 59 | 11.36 | 189.8 | 98.6 | 1.92 |
| | S5BN-0-9 | I | 6.00 | 0.10 | 0.65 | 0.57 | 3.50 | 43 | NW | GFRP | 1124 | 59 | 8.43 | 141.8 | 73.4 | 1.93 |
| | S7BH-0-13 | I | 6.00 | 0.10 | 0.65 | 0.56 | 3.57 | 75 | NW | GFRP | 1000 | 62.6 | 11.46 | 210.8 | 103.4 | 2.04 |
| | S9CN-0-17 | I | 6.00 | 0.10 | 0.65 | 0.57 | 3.50 | 37 | NW | GFRP | 1000 | 62.6 | 8.43 | 127.8 | 69.3 | 1.84 |
| Spadea et al. (2017) | I.1,2 | R | 1.20 | 0.11 | 0.22 | 0.20 | 2.50 | 35 | NW | CFRP | 2172 | 124 | 0.66 | 19.7 | 14.6 | 1.35 |
| Maranan et al. (2018) | GG-3.0-5 | R | 1.86 | 0.20 | 0.30 | 0.24 | 3.05 | 35 | NW | GFRP | 1184 | 62.6 | 2.10 | 63.9 | 40.5 | 1.58 |

$f'_c$ = concrete compressive strength; $E_f$, $f_{fu}$ = elastic modulus and tensile strength of FRP rebars, respectively

$\rho_f$ = longitudinal reinforcement ratio of FRP rebars

$L$, $b_w$, $h$, $d$ = span length, web width, height, and effective depth of the beams, respectively

Cross section: R = rectangular, T = T- shape, I = I-shape

Concrete type: NW = normal-weight concrete, LW = lightweight concrete

**Table 3** Database of FRP-RC beams with FRP shear reinforcement

| Authors | Specimen | Dimension and geometry of beams | | | | | | Concrete | | FRP type | Longitudinal reinforcement | | | Shear reinforcement | | | $V_{n,test}$ (kN) | $V_{n,KDS}$ (kN) | $V_{n,test}/V_{n,KDS}$ |
|---|---|---|---|---|---|---|---|---|---|---|---|---|---|---|---|---|---|---|---|
| | | Cross-section | $L$ (m) | $b_w$ (m) | $h$ (m) | $d$ (m) | $a/d$ | $f'_c$ (MPa) | Concrete type | | $f_{fu}$ (MPa) | $E_{fl}$ (GPa) | $\rho_{fl}$ (%) | $f_{fvu}$ (MPa) | $E_{fv}$ (GPa) | $\rho_{fv}$ (%) | | | |
| Maruyama and Zhao (1994) | FF1-20 | R | 3.00 | 0.15 | 0.30 | 0.25 | 3.00 | 36 | NW | CFRP | 1308 | 94.0 | 0.55 | 1308 | 94.0 | 0.12 | 61.6 | 48.4 | 1.27 |
| | FF2-10 | R | 3.00 | 0.15 | 0.30 | 0.25 | 3.00 | 33 | NW | CFRP | 1308 | 94.0 | 1.10 | 1308 | 94.0 | 0.24 | 91.6 | 80.7 | 1.13 |
| | FF1-10 | R | 3.00 | 0.15 | 0.30 | 0.25 | 3.00 | 38 | NW | CFRP | 1308 | 94.0 | 0.55 | 1308 | 94.0 | 0.24 | 86.6 | 74.4 | 1.16 |
| | FF3-10 | R | 3.00 | 0.15 | 0.30 | 0.25 | 3.00 | 31 | NW | CFRP | 1308 | 94.0 | 1.39 | 1308 | 94.0 | 0.24 | 97.6 | 83.9 | 1.16 |
| | FF2-20 | R | 3.00 | 0.15 | 0.30 | 0.25 | 3.00 | 35 | NW | CFRP | 1308 | 94.0 | 1.06 | 1308 | 94.0 | 0.12 | 75.4 | 56.3 | 1.34 |
| | FF4-10 | R | 3.00 | 0.15 | 0.30 | 0.25 | 3.00 | 31 | NW | CFRP | 1308 | 94.0 | 2.11 | 1308 | 94.0 | 0.24 | 122.1 | 93.3 | 1.31 |
| | FF4-13 | R | 3.00 | 0.15 | 0.30 | 0.25 | 3.00 | 31 | NW | CFRP | 1308 | 94.0 | 2.11 | 1308 | 94.0 | 0.18 | 88.6 | 75.8 | 1.17 |
| | FF4-16 | R | 3.00 | 0.15 | 0.30 | 0.25 | 3.00 | 31 | NW | CFRP | 1308 | 94.0 | 2.11 | 1308 | 94.0 | 0.15 | 77.6 | 68.0 | 1.14 |
| | FF4-20 | R | 3.00 | 0.15 | 0.30 | 0.25 | 3.00 | 35 | NW | CFRP | 1308 | 94.0 | 2.11 | 1308 | 94.0 | 0.12 | 85.1 | 65.3 | 1.30 |
| Okamoto et al. (1994) | AA1060M | R | 3.00 | 0.25 | 0.30 | 0.25 | 1.19 | 38 | NW | GFRP | 1167 | 61.0 | 1.90 | 1167 | 61.0 | 1.05 | 271.7 | 290.8 | 0.93 |
| | AA1060M-C | R | 3.00 | 0.25 | 0.30 | 0.25 | 1.19 | 37 | NW | GFRP | 1167 | 61.0 | 1.90 | 1167 | 61.0 | 1.05 | 252.1 | 287.6 | 0.88 |
| | AA1090M | R | 3.30 | 0.25 | 0.30 | 0.25 | 1.78 | 38 | NW | GFRP | 1167 | 61.0 | 1.90 | 1167 | 61.0 | 1.05 | 264.9 | 289.8 | 0.91 |
| | AC0512M | R | 3.60 | 0.25 | 0.30 | 0.25 | 1.78 | 33 | NW | GFRP | 1167 | 61.0 | 1.90 | 1167 | 61.0 | 0.51 | 158.9 | 165.7 | 0.96 |
| | AC1060M-C | R | 3.00 | 0.25 | 0.30 | 0.25 | 1.78 | 37 | NW | GFRP | 1167 | 61.0 | 1.90 | 1167 | 61.0 | 1.03 | 267.8 | 286.2 | 0.94 |
| | AC1060M | R | 3.00 | 0.25 | 0.30 | 0.25 | 1.19 | 38 | NW | GFRP | 1167 | 61.0 | 1.90 | 1167 | 61.0 | 1.03 | 278.6 | 288.0 | 0.97 |
| | AC1090M | R | 3.30 | 0.25 | 0.30 | 0.25 | 1.78 | 38 | NW | GFRP | 1167 | 61.0 | 1.90 | 1167 | 61.0 | 1.03 | 286.5 | 289.2 | 0.99 |
| | AC1012M | R | 3.60 | 0.25 | 0.30 | 0.25 | 1.78 | 33 | NW | GFRP | 1167 | 61.0 | 1.90 | 1167 | 61.0 | 1.03 | 229.6 | 278.7 | 0.82 |
| | AC1560M | R | 3.00 | 0.25 | 0.30 | 0.25 | 1.19 | 33 | NW | GFRP | 1167 | 61.0 | 1.90 | 1167 | 61.0 | 1.05 | 359.0 | 288.6 | 1.24 |
| | AC1590L | R | 3.30 | 0.25 | 0.30 | 0.25 | 1.78 | 29 | NW | GFRP | 1167 | 61.0 | 1.90 | 1167 | 61.0 | 1.05 | 217.8 | 279.1 | 0.78 |
| | AC1512M | R | 3.60 | 0.25 | 0.30 | 0.25 | 2.37 | 33 | NW | GFRP | 1167 | 61.0 | 1.90 | 1167 | 61.0 | 1.05 | 262.9 | 287.8 | 0.91 |
| Nakamura and Higai (1995) | GG05-10 | R | 1.50 | 0.20 | 0.30 | 0.25 | 3.00 | 35 | NW | GFRP | 751 | 29.4 | 1.61 | 828 | 31.0 | 0.35 | 83.9 | 62.8 | 1.34 |
| | GG10-10 | R | 1.50 | 0.20 | 0.30 | 0.25 | 3.00 | 33 | NW | GFRP | 751 | 29.4 | 1.61 | 828 | 31.4 | 0.35 | 100.6 | 65.9 | 1.53 |
| | GG05-20 | R | 1.50 | 0.20 | 0.30 | 0.25 | 3.00 | 35 | NW | GFRP | 751 | 29.4 | 1.61 | 828 | 31.0 | 0.18 | 56.0 | 43.7 | 1.28 |
| | GG10-20 | R | 1.50 | 0.20 | 0.30 | 0.25 | 3.00 | 35 | NW | GFRP | 751 | 29.4 | 1.61 | 828 | 31.0 | 0.18 | 66.0 | 45.9 | 1.44 |
| Zhao et al. (1995) | #10 | R | 1.80 | 0.15 | 0.30 | 0.25 | 3.00 | 34 | NW | CFRP | 1124 | 105.0 | 3.03 | 1100 | 39.0 | 0.42 | 114.3 | 86.9 | 1.32 |
| | #14 | R | 1.80 | 0.15 | 0.30 | 0.25 | 3.00 | 34 | NW | CFRP | 1124 | 105.0 | 3.03 | 1300 | 39.0 | 0.42 | 127.2 | 89.7 | 1.42 |
| | #16 | R | 1.80 | 0.15 | 0.30 | 0.25 | 3.00 | 34 | NW | CFRP | 1124 | 105.0 | 2.27 | 1100 | 39.0 | 0.42 | 117.5 | 83.8 | 1.40 |
| | #19 | R | 2.00 | 0.15 | 0.30 | 0.25 | 4.00 | 34 | NW | CFRP | 1124 | 105.0 | 1.51 | 1100 | 39.0 | 0.42 | 74.4 | 69.8 | 1.07 |
| Maruyama (1996) | #25 | R | 1.80 | 0.15 | 0.30 | 0.25 | 2.50 | 34 | NW | CFRP | 1200 | 100.0 | 1.51 | 600 | 30.0 | 0.43 | 109.9 | 70.3 | 1.56 |

**Table 3** (continued)

| Authors | Specimen | Dimension and geometry of beams | | | | | | Concrete | | FRP type | Longitudinal reinforcement | | | Shear reinforcement | | | $V_{n,test}$ (kN) | $V_{n,KDS}$ (kN) | $V_{n,test}$/ $V_{n,KDS}$ |
|---|---|---|---|---|---|---|---|---|---|---|---|---|---|---|---|---|---|---|---|
| | | Cross-section | $L$ (m) | $b_w$ (m) | $h$ (m) | $d$ (m) | $a/d$ | $f'_c$ (MPa) | Concrete type | | $f_{fu}$ (MPa) | $E_{fl}$ (GPa) | $\rho_{fl}$ (%) | $f_{fvu}$ (MPa) | $E_{fv}$ (GPa) | $\rho_{fv}$ (%) | | | |
| | #26 | R | 1.80 | 0.15 | 0.30 | 0.25 | 2.50 | 34 | NW | CFRP | 1200 | 100.0 | 1.51 | 600 | 30.0 | 0.43 | 109.9 | 70.3 | 1.56 |
| | #27 | R | 1.80 | 0.15 | 0.30 | 0.25 | 2.50 | 34 | NW | CFRP | 1200 | 100.0 | 1.51 | 600 | 30.0 | 0.86 | 140.9 | 100.2 | 1.41 |
| | #28 | R | 1.80 | 0.15 | 0.30 | 0.25 | 2.50 | 34 | NW | CFRP | 1200 | 100.0 | 1.51 | 600 | 30.0 | 0.86 | 140.9 | 100.2 | 1.41 |
| | #30 | R | 2.50 | 0.30 | 0.55 | 0.50 | 2.50 | 34 | NW | CFRP | 1200 | 100.0 | 1.04 | 600 | 30.0 | 0.43 | 375.4 | 228.3 | 1.64 |
| | #32 | R | 3.75 | 0.45 | 0.80 | 0.75 | 2.50 | 34 | NW | CFRP | 1200 | 100.0 | 1.04 | 600 | 30.0 | 0.43 | 607.7 | 448.0 | 1.36 |
| Vijay et al. (1996) | S2 | R | 0.00 | 0.15 | 0.30 | 0.27 | 1.89 | 45 | NW | GFRP | 655 | 54.0 | 1.43 | 655 | 54.0 | 0.83 | 127.8 | 133.4 | 0.96 |
| | S3 | R | 0.00 | 0.15 | 0.30 | 0.27 | 1.89 | 45 | NW | GFRP | 655 | 54.0 | 1.43 | 655 | 54.0 | 0.56 | 116.0 | 102.4 | 1.13 |
| | S5 | R | 0.00 | 0.15 | 0.30 | 0.27 | 1.89 | 31 | NW | GFRP | 655 | 54.0 | 0.67 | 655 | 54.0 | 0.83 | 124.2 | 120.0 | 1.04 |
| | S6 | R | 0.00 | 0.15 | 0.30 | 0.27 | 1.89 | 31 | NW | GFRP | 655 | 54.0 | 0.67 | 655 | 54.0 | 0.56 | 124.3 | 91.0 | 1.37 |
| Duranovic et al., (1997) | GB 11 | R | 0.00 | 0.15 | 0.25 | 0.21 | 3.65 | 40 | NW | GFRP | 1000 | 45.0 | 1.36 | 1000 | 45.0 | 0.17 | 49.8 | 36.9 | 1.35 |
| | GB 12 | R | 0.00 | 0.15 | 0.25 | 0.21 | 2.44 | 40 | NW | GFRP | 1000 | 45.0 | 1.36 | 1000 | 45.0 | 0.17 | 67.4 | 40.6 | 1.66 |
| Alsayed (1998) | B1 | R | 2.20 | 0.20 | 0.36 | 0.32 | 3.13 | 36 | NW | GFRP | 764 | 42.0 | 1.33 | 565 | 43.0 | 0.21 | 70.9 | 66.3 | 1.07 |
| Shehata et al. (2000) | CC-3 | T | 5.00 | 0.14 | 0.56 | 0.47 | 3.19 | 50 | NW | CFRP | 2200 | 137.0 | 1.25 | 1730 | 137.0 | 0.36 | 309.8 | 248.7 | 1.25 |
| | CG-3 | T | 5.00 | 0.14 | 0.56 | 0.47 | 3.19 | 50 | NW | CFRP | 2200 | 137.0 | 1.25 | 640 | 41.0 | 1.07 | 309.3 | 231.3 | 1.34 |
| Alkhrdaji et al. (2001) | BM1 | R | 1.50 | 0.18 | 0.33 | 0.28 | 2.69 | 24 | NW | GFRP | 717 | 40.0 | 2.30 | 717 | 40.0 | 0.52 | 82.4 | 90.1 | 0.91 |
| | BM2 | R | 1.50 | 0.18 | 0.33 | 0.28 | 2.69 | 24 | NW | GFRP | 717 | 40.0 | 2.30 | 717 | 40.0 | 0.39 | 71.8 | 74.9 | 0.96 |
| | BM5 | R | 1.50 | 0.18 | 0.33 | 0.28 | 2.69 | 25 | NW | GFRP | 717 | 40.0 | 2.30 | 717 | 40.0 | 0.52 | 81.6 | 90.2 | 0.90 |
| | BM6 | R | 1.50 | 0.18 | 0.33 | 0.28 | 2.69 | 25 | NW | GFRP | 717 | 40.0 | 1.19 | 717 | 40.0 | 0.39 | 53.5 | 65.7 | 0.81 |
| Niewels (2008) | Q-C-1R | R | 2.66 | 0.30 | 0.55 | 0.44 | 3.02 | 48 | NW | GFRP | 1000 | 63.0 | 3.65 | 322 | 31.0 | 0.54 | 364.7 | 271.1 | 1.35 |
| | Q-C-2R | R | 3.96 | 0.30 | 0.55 | 0.44 | 3.02 | 43 | NW | GFRP | 1000 | 63.0 | 3.65 | 322 | 31.0 | 0.38 | 245.4 | 210.4 | 1.17 |
| | Q-A-3R | R | 3.90 | 0.30 | 0.50 | 0.41 | 3.16 | 43 | NW | GFRP | 480 | 44.0 | 3.25 | 1000 | 49.0 | 0.30 | 305.8 | 217.7 | 1.40 |
| | Q-A-4R | R | 3.90 | 0.30 | 0.50 | 0.41 | 3.16 | 47 | NW | GFRP | 480 | 44.0 | 3.25 | 1000 | 49.0 | 0.24 | 270.8 | 194.4 | 1.39 |
| Ascione et al. (2010) | I.1.2.3.4.5 | R | 2.00 | 0.15 | 0.20 | 0.17 | 4.12 | 20 | NW | GFRP | 970 | 46.0 | 0.62 | 970 | 46.0 | 0.29 | 21.0 | 28.2 | 0.74 |
| | II.1.2.3.4.5 | R | 2.00 | 0.15 | 0.20 | 0.17 | 4.12 | 20 | NW | GFRP | 970 | 46.0 | 1.54 | 970 | 46.0 | 0.29 | 29.1 | 33.5 | 0.87 |
| | III.1.2.3.4.5 | R | 2.00 | 0.15 | 0.20 | 0.17 | 4.12 | 25 | NW | GFRP | 970 | 46.0 | 0.62 | 970 | 46.0 | 0.29 | 24.0 | 29.3 | 0.82 |
| | IV.1.2.3.4.5 | R | 2.00 | 0.15 | 0.20 | 0.17 | 4.12 | 25 | NW | GFRP | 970 | 46.0 | 1.54 | 970 | 46.0 | 0.29 | 33.9 | 35.2 | 0.96 |
| | V.1.2.3.4.5 | R | 2.00 | 0.15 | 0.20 | 0.17 | 4.12 | 20 | NW | CFRP | 2000 | 115.0 | 0.89 | 2000 | 115.0 | 0.29 | 39.8 | 63.3 | 0.63 |
| | VII.1.2.3.4.5 | R | 2.00 | 0.15 | 0.20 | 0.17 | 4.12 | 25 | NW | CFRP | 2000 | 115.0 | 0.89 | 2000 | 115.0 | 0.29 | 40.3 | 64.1 | 0.63 |

**Table 3** (continued)

| Authors | Specimen | Dimension and geometry of beams | | | | | | Concrete | | FRP type | Longitudinal reinforcement | | | Shear reinforcement | | | $V_{n,test}$ (kN) | $V_{n,KDS}$ (kN) | $V_{n,test}/V_{n,KDS}$ |
|---|---|---|---|---|---|---|---|---|---|---|---|---|---|---|---|---|---|---|---|
| | | Cross-section | $L$ (m) | $b_w$ (m) | $h$ (m) | $d$ (m) | $a/d$ | $f'_c$ (MPa) | Concrete type | | $f_{fu}$ (MPa) | $E_{fl}$ (GPa) | $\rho_{fl}$ (%) | $f_{fvu}$ (MPa) | $E_{fv}$ (GPa) | $\rho_{fv}$ (%) | | | |
| Bentz et al. (2010) | L20-1 | R | 7.10 | 0.45 | 1.00 | 0.86 | 3.56 | 36 | NW | GFRP | 397 | 37.1 | 2.23 | 397 | 40.8 | 0.09 | 425.0 | 268.8 | 1.58 |
| | L20-2 | R | 7.10 | 0.45 | 1.00 | 0.86 | 3.56 | 42 | NW | GFRP | 397 | 37.1 | 2.23 | 397 | 40.8 | 0.19 | 675.0 | 391.5 | 1.72 |
| | M20-1 | R | 3.05 | 0.45 | 0.50 | 0.41 | 3.77 | 35 | NW | GFRP | 397 | 37.1 | 2.36 | 397 | 40.8 | 0.09 | 151.5 | 149.9 | 1.01 |
| Tomlinson and Fam (2015) | FT | R | 2.90 | 0.15 | 0.30 | 0.27 | 4.07 | 51 | NW | BFRP | 1100 | 70.0 | 0.39 | 1100 | 70.0 | 0.17 | 37.4 | 45.5 | 0.82 |
| | FB | R | 2.90 | 0.15 | 0.30 | 0.27 | 4.07 | 53 | NW | BFRP | 1100 | 70.0 | 0.51 | 1100 | 70.0 | 0.17 | 45.9 | 47.4 | 0.97 |
| | FC | R | 2.90 | 0.15 | 0.30 | 0.25 | 4.49 | 52 | NW | BFRP | 1100 | 70 | 0.85 | 1100 | 70.0 | 0.168 | 54.50 | 49.6 | 1.10 |
| Kurth (2012) | S1AN-1.3-2 | I | 6.00 | 0.10 | 0.65 | 0.566 | 3.53 | 38 | NW | GFRP | 1124 | 59 | 8.52 | 1000 | 56.2 | 1.26 | 435.60 | 320.4 | 1.36 |
| | S2AN-0.8-3 | I | 6.00 | 0.10 | 0.65 | 0.566 | 3.53 | 34 | NW | GFRP | 1124 | 59 | 8.52 | 1000 | 56.2 | 0.75 | 340.60 | 224.3 | 1.52 |
| | S2AN-2.3-4 | I | 6.00 | 0.10 | 0.65 | 0.566 | 3.53 | 34 | NW | GFRP | 1124 | 59 | 8.52 | 1000 | 56.2 | 2.26 | 494.60 | 473.9 | 1.04 |
| | S3AH-1.3-6 | I | 6.00 | 0.10 | 0.65 | 0.566 | 3.53 | 82 | NW | GFRP | 1124 | 59 | 11.36 | 1000 | 56.2 | 1.26 | 579.60 | 365.1 | 1.59 |
| | S4AH-0.8-7 | I | 6.00 | 0.10 | 0.65 | 0.566 | 3.53 | 42 | NW | GFRP | 1124 | 59 | 11.36 | 1000 | 56.2 | 0.75 | 334.60 | 233.8 | 1.43 |
| | S4AH-2.3-8 | I | 6.00 | 0.10 | 0.65 | 0.566 | 3.53 | 43 | NW | GFRP | 1124.00 | 59.00 | 11.36 | 1000 | 56.2 | 2.26 | 553 | 503.9 | 1.10 |
| | S5BN-1.3-10 | I | 6.00 | 0.10 | 0.65 | 0.57 | 3.50 | 43 | NW | GFRP | 1124 | 59.0 | 8.43 | 1000 | 57.0 | 1.26 | 447.6 | 329.4 | 1.36 |
| | S6BN-0.8-11 | I | 6.00 | 0.10 | 0.65 | 0.57 | 3.50 | 30 | NW | GFRP | 1000 | 62.6 | 8.43 | 1000 | 57.0 | 0.75 | 310.6 | 222.2 | 1.40 |
| | S6BN-2.3-12 | I | 6.00 | 0.10 | 0.65 | 0.57 | 3.50 | 31 | NW | GFRP | 1000 | 62.6 | 8.43 | 1000 | 57.0 | 2.26 | 456.6 | 479.8 | 0.95 |
| | S7BH-1.3-14 | I | 6.00 | 0.10 | 0.65 | 0.56 | 3.57 | 76 | NW | GFRP | 1000 | 62.6 | 11.46 | 1000 | 57.0 | 1.26 | 634.6 | 373.5 | 1.70 |
| | S8BH-0.8-15 | I | 6.00 | 0.10 | 0.65 | 0.56 | 3.57 | 73 | NW | GFRP | 1000 | 62.6 | 11.46 | 1000 | 57.0 | 0.75 | 447.6 | 264.9 | 1.69 |
| | S8BH-2.3-16 | I | 6.00 | 0.10 | 0.65 | 0.56 | 3.57 | 70 | NW | GFRP | 1000 | 62.6 | 11.46 | 1000 | 57.0 | 2.26 | 589.6 | 525.4 | 1.12 |
| Matta et al. (2013) | S1-0.12-MA | R | 7.32 | 0.46 | 0.98 | 0.88 | 3.10 | 39 | NW | GFRP | 476 | 41.0 | 0.60 | 690 | 40.2 | 0.22 | 290.3 | 319.8 | 0.91 |
| Krall (2014) | BM12-220 | R | 1.35 | 0.20 | 0.33 | 0.27 | 2.50 | 47 | NW | GFRP | 1000 | 60.0 | 1.82 | 900 | 50.0 | 0.51 | 191.8 | 137.8 | 1.39 |
| | BM12-150 | R | 1.35 | 0.20 | 0.33 | 0.27 | 2.50 | 47 | NW | GFRP | 1000 | 60.0 | 1.82 | 900 | 50.0 | 0.75 | 203.2 | 172.0 | 1.18 |
| | BM16-220 | R | 1.35 | 0.20 | 0.35 | 0.27 | 2.50 | 47 | NW | GFRP | 1000 | 60.0 | 2.23 | 900 | 50.0 | 0.51 | 155.2 | 134.6 | 1.15 |
| | BM16-150 | R | 1.35 | 0.20 | 0.35 | 0.27 | 2.50 | 47 | NW | GFRP | 1000 | 60.0 | 2.23 | 900 | 50.0 | 0.75 | 208.8 | 176.6 | 1.18 |
| | BM25-220 | R | 1.35 | 0.20 | 0.35 | 0.27 | 2.50 | 47 | NW | GFRP | 1000 | 60.0 | 2.51 | 900 | 50.0 | 0.51 | 180.6 | 141.4 | 1.28 |
| | BM25-150 | R | 1.35 | 0.20 | 0.35 | 0.27 | 2.50 | 47 | NW | GFRP | 1000 | 60.0 | 2.51 | 900 | 50.0 | 0.75 | 208.5 | 178.8 | 1.17 |
| | BM25-s230 | R | 1.35 | 0.23 | 0.35 | 0.27 | 2.50 | 47 | NW | GFRP | 1000 | 60.0 | 1.58 | 900 | 50.0 | 1.19 | 234.1 | 263.4 | 0.89 |
| | BM16-s230 | R | 1.35 | 0.23 | 0.36 | 0.27 | 2.50 | 47 | NW | GFRP | 1000 | 60.0 | 1.94 | 900 | 50.0 | 1.19 | 225.7 | 266.1 | 0.85 |
| | BM12-s230 | R | 1.35 | 0.23 | 0.37 | 0.27 | 2.50 | 47 | NW | GFRP | 1000 | 60.0 | 2.18 | 900 | 50.0 | 1.19 | 222.7 | 268.0 | 0.83 |
| Johnson (2014) | JSC32-22B | R | 3.36 | 0.40 | 0.65 | 0.58 | 2.92 | 32 | NW | GFRP | 1204 | 61.2 | 1.04 | 911 | 57.5 | 0.28 | 392.5 | 328.2 | 1.20 |

**Table 3** (continued)

| Authors | Specimen | Dimension and geometry of beams | | | | | | Concrete | | FRP type | Longitudinal reinforcement | | | Shear reinforcement | | | $V_{n,test}$ (kN) | $V_{n,KDS}$ (kN) | $V_{n,test}/V_{n,KDS}$ |
|---|---|---|---|---|---|---|---|---|---|---|---|---|---|---|---|---|---|---|---|
| | | Cross-section | $L$ (m) | $b_w$ (m) | $h$ (m) | $d$ (m) | $a/d$ | $f'_c$ (MPa) | Concrete type | | $f_{fu}$ (MPa) | $E_{fl}$ (GPa) | $\rho_{fl}$ (%) | $f_{fvu}$ (MPa) | $E_{fv}$ (GPa) | $\rho_{fv}$ (%) | | | |
| | JSC32-40B | R | 3.36 | 0.40 | 0.65 | 0.58 | 2.92 | 32 | NW | GFRP | 1204 | 61.2 | 1.04 | 911 | 57.5 | 0.37 | 456.0 | 397.9 | 1.15 |
| | JSC32-50B | R | 3.36 | 0.40 | 0.65 | 0.58 | 2.92 | 32 | NW | GFRP | 1204 | 61.2 | 1.04 | 911 | 57.5 | 0.50 | 553.0 | 498.1 | 1.11 |
| | JSV40-22B | R | 3.36 | 0.40 | 0.65 | 0.58 | 2.92 | 40 | NW | GFRP | 1264 | 71.2 | 1.03 | 655 | 41.5 | 0.32 | 380.0 | 303.8 | 1.25 |
| | JSV40-40B | R | 3.36 | 0.40 | 0.65 | 0.58 | 2.92 | 40 | NW | GFRP | 1264 | 71.2 | 1.03 | 655 | 41.5 | 0.42 | 453.0 | 364.0 | 1.24 |
| | JSV40-50B | R | 3.36 | 0.40 | 0.65 | 0.58 | 2.92 | 40 | NW | GFRP | 1264 | 71.2 | 1.03 | 655 | 41.5 | 0.57 | 539.0 | 449.1 | 1.20 |
| | JSC100-50B | R | 3.36 | 0.40 | 0.65 | 0.58 | 2.92 | 102 | NW | GFRP | 1204 | 61.2 | 1.04 | 911 | 57.5 | 0.50 | 565.5 | 530.0 | 1.07 |
| Issa et al. (2016) | 2-13SB1 | R | 3.05 | 0.20 | 0.30 | 0.28 | 1.50 | 36 | NW | BFRP | 1060 | 51.0 | 0.50 | 1070 | 53.0 | 0.54 | 149.1 | 117.6 | 1.27 |
| | 3-13SB1 | R | 3.05 | 0.20 | 0.30 | 0.28 | 1.50 | 36 | NW | BFRP | 1060 | 51.0 | 0.75 | 1070 | 53.0 | 0.54 | 197.4 | 125.5 | 1.57 |
| | 3-16SB1 | R | 3.05 | 0.20 | 0.30 | 0.27 | 1.50 | 36 | NW | BFRP | 1060 | 51.0 | 1.17 | 1070 | 53.0 | 0.54 | 215.6 | 133.8 | 1.61 |
| | 2-25B1 | R | 3.05 | 0.20 | 0.30 | 0.27 | 1.50 | 36 | NW | BFRP | 1060 | 51.0 | 1.92 | 1070 | 53.0 | 0.54 | 193.7 | 140.4 | 1.38 |
| | 3-16B2 | R | 3.05 | 0.20 | 0.30 | 0.27 | 2.50 | 36 | NW | BFRP | 1060 | 51.0 | 1.17 | 1070 | 53.0 | 0.54 | 136.5 | 125.9 | 1.08 |
| | 3-16B3 | R | 3.05 | 0.20 | 0.30 | 0.27 | 3.50 | 36 | NW | BFRP | 1060 | 51.0 | 1.17 | 1070 | 53.0 | 0.54 | 93.1 | 118.0 | 0.79 |
| Maranan et al. (2018) | GG-3.0-5-S75 | R | 1.86 | 0.20 | 0.30 | 0.24 | 3.05 | 35 | NW | GFRP | 1184 | 62.6 | 2.10 | 1029 | 50.0 | 0.95 | 202.4 | 180.5 | 1.12 |
| | GG-3.0-5-S100 | R | 1.86 | 0.20 | 0.30 | 0.24 | 3.05 | 35 | NW | GFRP | 1184 | 62.6 | 2.10 | 1029 | 50.0 | 0.72 | 187.4 | 150.9 | 1.24 |
| | GG-3.0-5-S150 | R | 1.86 | 0.20 | 0.30 | 0.24 | 3.05 | 35 | NW | GFRP | 1184 | 62.6 | 2.10 | 1029 | 50.0 | 0.48 | 150.4 | 116.1 | 1.30 |
| | GG-3.0-5-C100 | R | 1.86 | 0.20 | 0.30 | 0.24 | 3.05 | 35 | NW | GFRP | 1184 | 62.6 | 2.10 | 1029 | 50.0 | 0.72 | 156.4 | 145.6 | 1.07 |
| Imjai (2007) | TB2B | R | 2.30 | 0.15 | 0.25 | 0.22 | 3.50 | 48 | NW | GFRP | 1000 | 60.0 | 1.22 | 720 | 27.9 | 0.37 | 66.5 | 47.8 | 1.39 |
| | TB4B | R | 2.30 | 0.15 | 0.25 | 0.22 | 3.50 | 48 | NW | GFRP | 750 | 45.0 | 1.30 | 720 | 27.9 | 0.36 | 60.0 | 44.4 | 1.35 |
| | TB5B | R | 2.30 | 0.15 | 0.25 | 0.22 | 3.50 | 48 | NW | GFRP | 750 | 45.0 | 1.30 | 720 | 27.9 | 0.48 | 67.8 | 51.5 | 1.32 |
| Yang (2014) | GB50-P150 | R | 2.30 | 0.15 | 0.25 | 0.22 | 3.52 | 35 | NW | GFRP | 758 | 46.0 | 0.81 | 720 | 27.9 | 0.27 | 30.7 | 30.3 | 1.01 |
| | CB51-P150 | R | 2.30 | 0.15 | 0.25 | 0.22 | 3.52 | 35 | NW | CFRP | 758 | 124.0 | 0.81 | 720 | 27.9 | 0.27 | 42.6 | 38.6 | 1.10 |
| | GB52-P80 | R | 1.80 | 0.15 | 0.25 | 0.22 | 2.75 | 35 | NW | GFRP | 2068 | 46.0 | 0.81 | 720 | 27.9 | 0.50 | 47.7 | 44.1 | 1.08 |
| Grace et al. (2015) | C000-C4-3 | I | 1.22 | 0.08 | 0.41 | 0.37 | 3.00 | 62 | NW | CFRP | 2930 | 149.0 | 2.92 | 2840 | 150.0 | 0.98 | 208.3 | 272.2 | 0.77 |
| Spadea et al. (2017) | II.1.2 | R | 1.20 | 0.11 | 0.22 | 0.20 | 2.50 | 35 | NW | CFRP | 2172 | 124.0 | 0.66 | 1313 | 100.8 | 0.13 | 60.3 | 37.5 | 1.61 |

$f'_c$ = concrete compressive strength; $E_{fl}$, $f_{fu}$, $\rho_{fl}$ = elastic modulus, tensile strength, and reinforcement ratio of FRP longitudinal rebars, respectively. $E_{fv}$, $f_{fvu}$, $\rho_{fv}$ = elastic modulus, tensile strength, and reinforcement ratio of FRP shear rebars, respectively. $L$, $b_w$, $h$, $d$ = span length, web width, height, and effective depth of the beams, respectively. Cross section: R = rectangular, T = T-shape, I = I-shape. Concrete type: NW = normal-weight concrete, LW = lightweight concrete

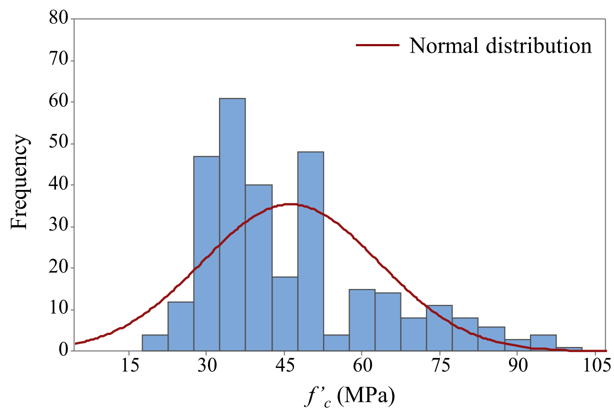


(a) According to concrete compressive strength

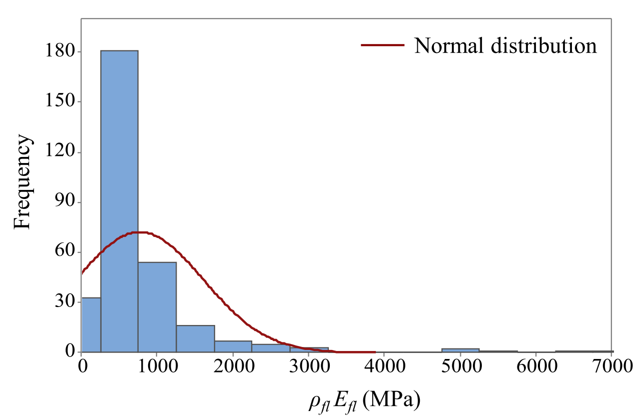


(b) According to FRP axial stiffness

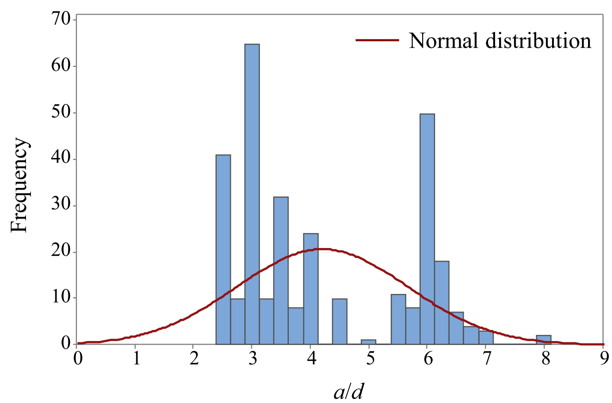


(c) According to *a*/*d* ratio

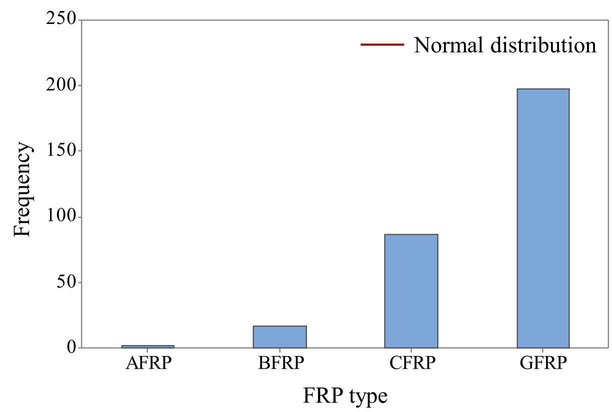


(d) According to FRP type

**Fig. 2** Distribution of design parameters for the database of specimens without stirrups (304 specimens)

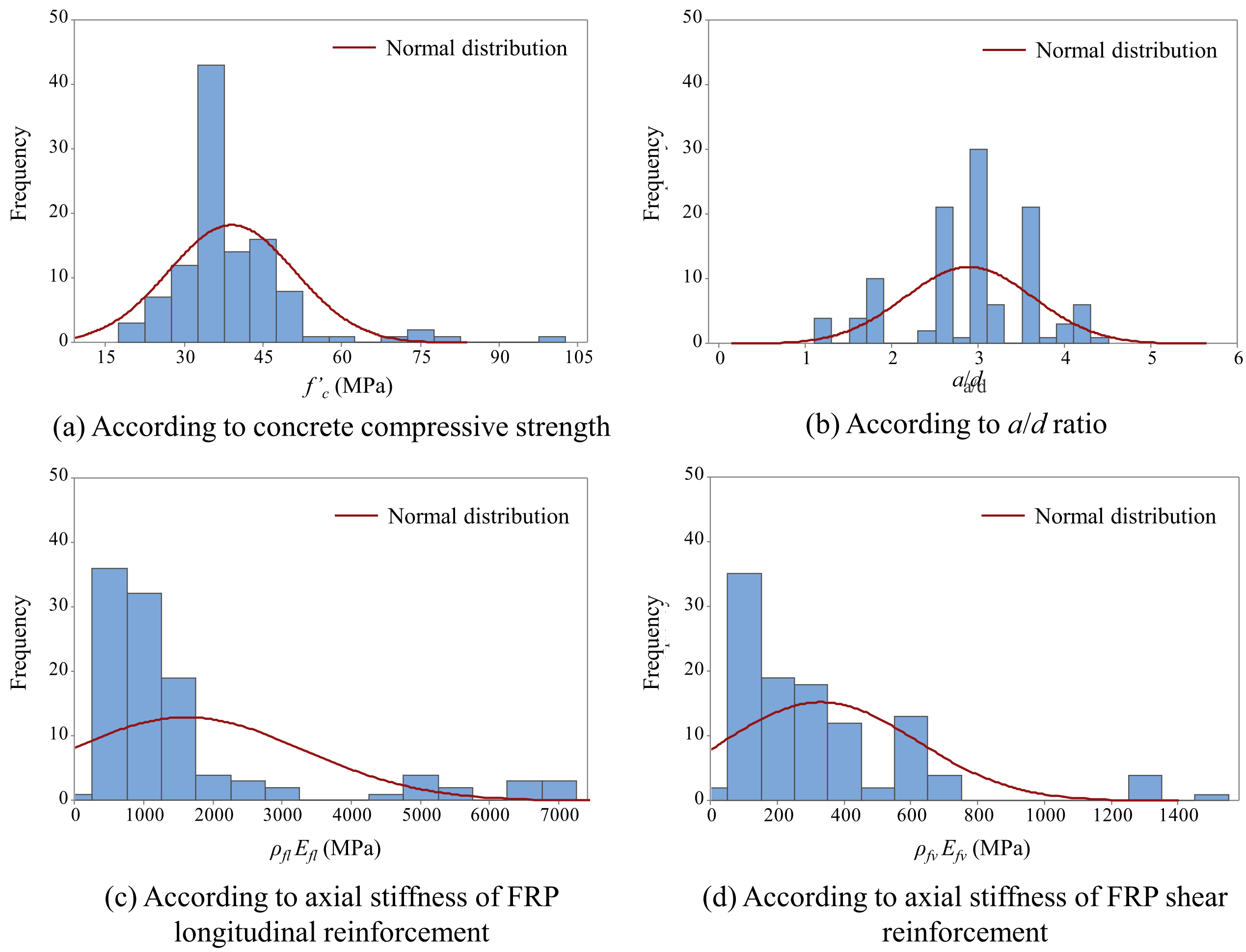


**Fig. 3** Distribution of design parameters for the database of specimens with stirrups (110 specimens)

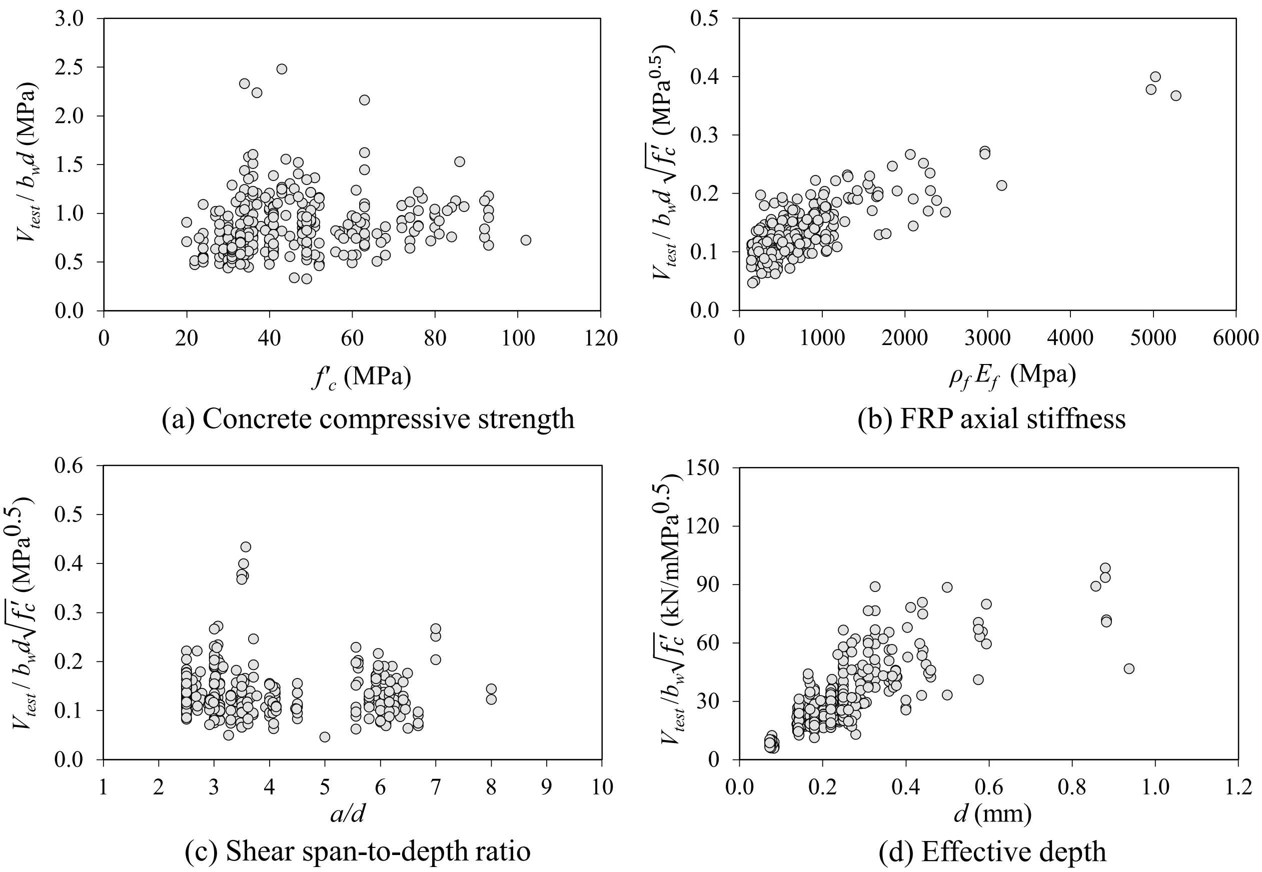


**Fig. 4** Effect of primary design parameters on the normalized one-way shear strength of FRP-RC specimens

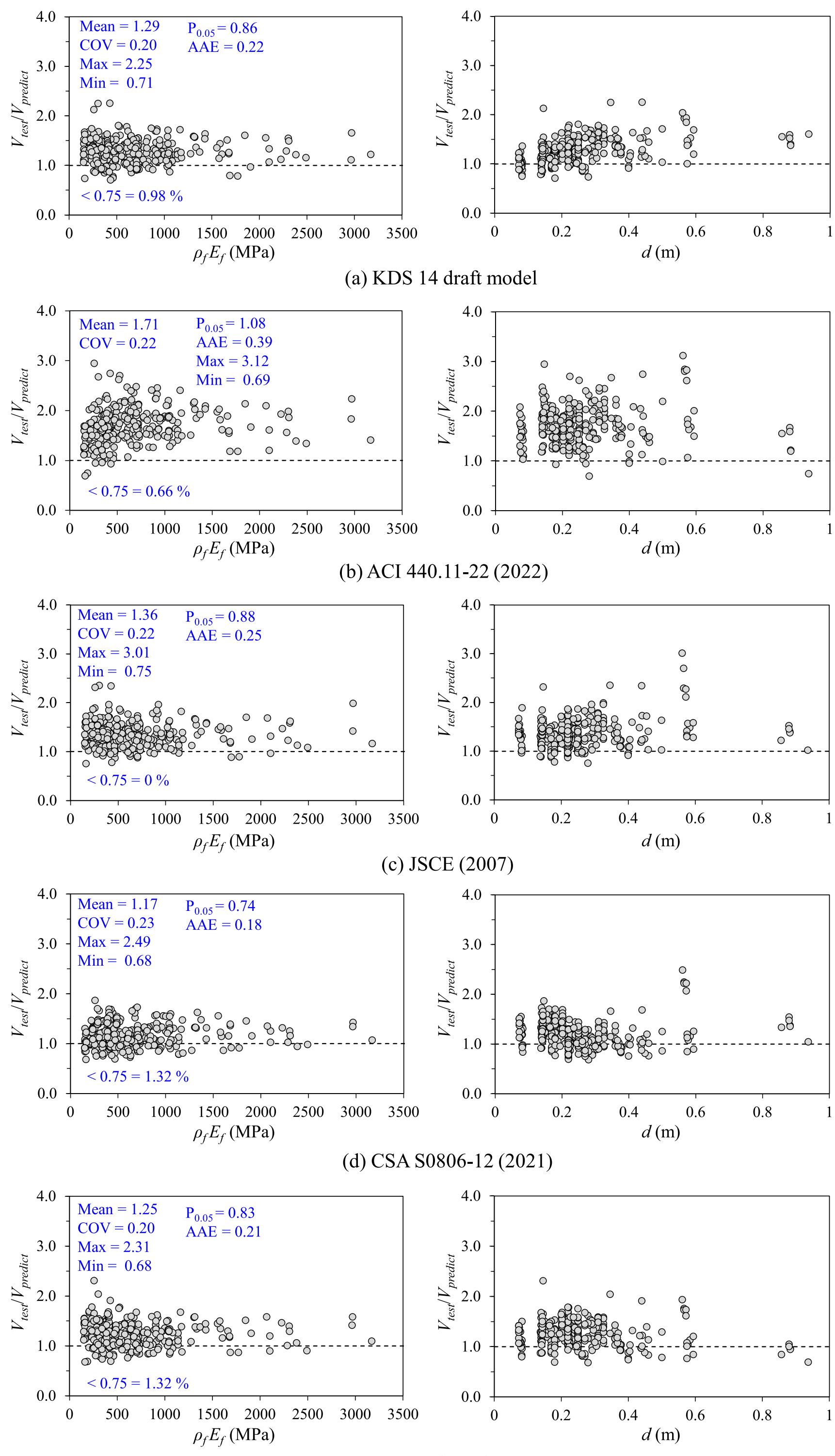


**Fig. 5** Comparative analysis of the shear strength ratios using different design codes for specimens without FRP stirrups

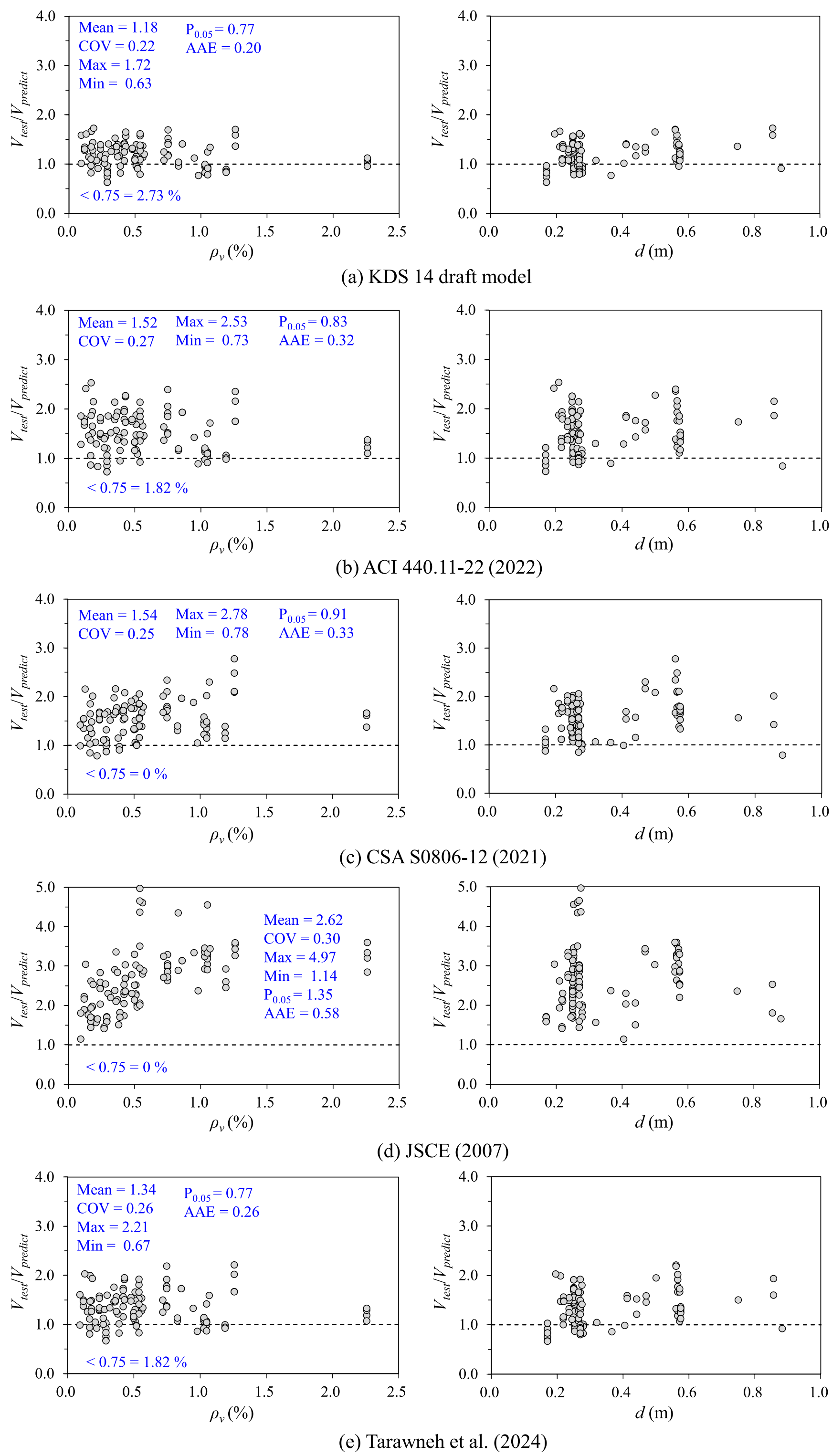


**Fig. 6** Comparative analysis of the shear strength ratios using different design codes for specimens with FRP stirrups

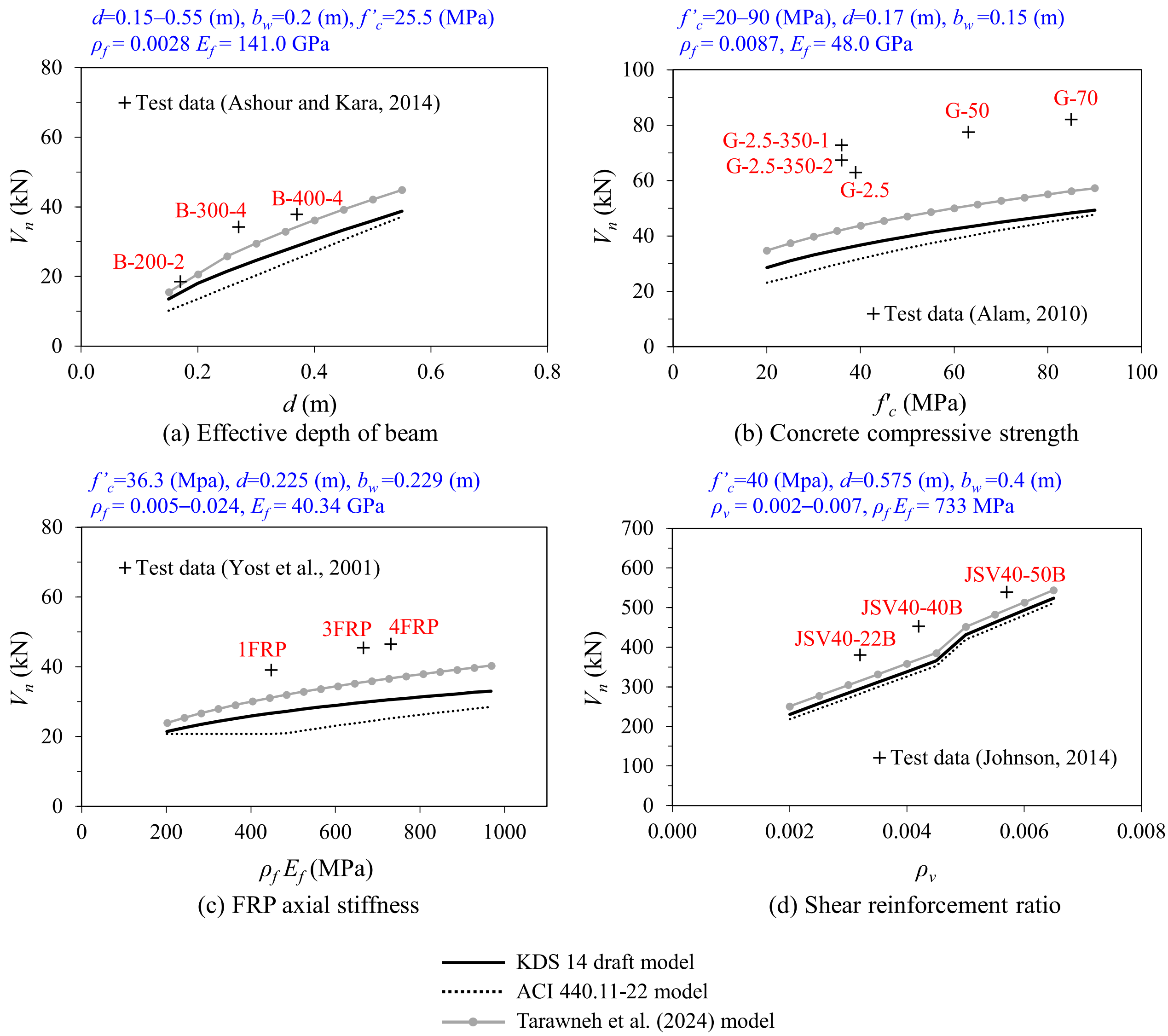


**Fig. 7** Parametric study using KDS 14 draft and existing design models

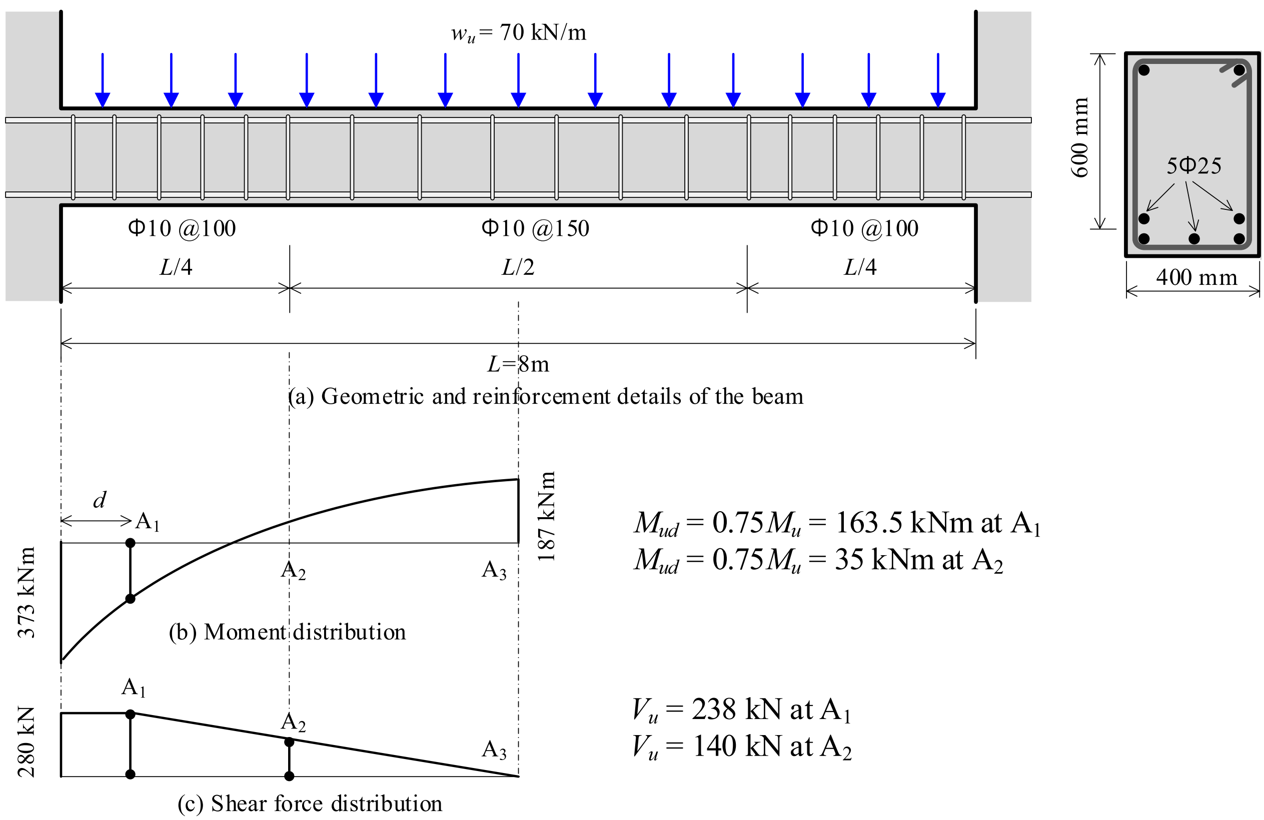


**Fig. 8** Shear design example for FRP-RC beam using the KDS 14 draft model

## Appendix: Database for one-way shear tests of FRP-RC members.

See Tables 2, 3.

**Acknowledgements**
The authors gratefully acknowledge the financial support provided by the Basic Science Research Program of the National Research Foundation of Korea (Grant nos. NRF-2022R1A2C2004351 and NRF-2020R1A6A1A03044977).

**Author Contributions**
N.H.D: conceptualization, methodology, data curation, writing–original draft. S.-H. K: data curation, investigation. K.-K. C: conceptualization, writing–original draft, review and editing, funding acquisition. All the authors read and approved the final manuscript.

**Availability of Data and Materials**
The authors declare that the datasets used or analyzed during the current study are available from the corresponding author on reasonable request.

## Declarations

**Ethics Approval and Consent to Participate**
Not applicable.

**Consent for Publication**
Not applicable.

**Competing Interests**
The authors declare no competing interests.

Received: 20 November 2024 Accepted: 18 May 2025
Published online: 07 August 2025

**References**

Acciai, A., D'Ambrisi, A., De Stefano, M., Feo, L., Focacci, F., & Nudo, R. (2016). Experimental response of FRP reinforced members without transverse reinforcement: Failure modes and design issues. *Composites Part B: Engineering, 89*, 397–407. https://doi.org/10.1016/j.compositesb.2016.01.002

ACI Committee, and International Organization for Standardization. (2019). ACI 318-19: Building code requirements for structural concrete and commentary. American Concrete Institute.

ACI Committee 440. (2022). Building Code Requirements for Structural Concrete Reinforced with Glass Fiber-Reinforced Polymer (GFRP) Bars—Code and Commentary. ACI 440.11–22. Farmington Hills: American Concrete Institute.

Alam, M. S. (2010). *Influence of different parameters on shear strength of FRP reinforced concrete beams without web reinforcement* (Doctoral dissertation, Memorial University of Newfoundland).

Alam, M. S., & Hussein, A. (2011). Experimental investigation on the effect of longitudinal reinforcement on shear strength of fibre reinforced polymer reinforced concrete beams. *Canadian Journal of Civil Engineering, 38*(3), 243–251. https://doi.org/10.1139/L10-126

Alkhrdaji, T., Wideman, M., Belarbi, A., & Nanni, A. (2001, October). Shear strength of GFRP RC beams and slabs. In *Proceedings of the international conference, composites in construction-CCC*. Porto, Portugal (pp. 409–414).

Alsayed, S. H. (1998). Flexural behaviour of concrete beams reinforced with GFRP bars. *Cement and Concrete Composites, 20*(1), 1–11. https://doi.org/10.1016/S0958-9465(97)00061-9

Ascione, L., Mancusi, G., & Spadea, S. (2010). Flexural behaviour of concrete beams reinforced with GFRP bars. *Strain, 46*(5), 460–469. https://doi.org/10.1111/j.1475-1305.2009.00662.x

Ashour, A. F. (2006). Flexural and shear capacities of concrete beams reinforced with GFRP bars. *Construction and Building Materials, 20*(10), 1005–1015. https://doi.org/10.1016/j.conbuildmat.2005.06.023

Ashour, A. F., & Kara, I. F. (2014). Size effect on shear strength of FRP reinforced concrete beams. *Composites Part B: Engineering, 60*, 612–620. https://doi.org/10.1016/j.compositesb.2013.12.002

Bentz, E. C., Massam, L., & Collins, M. P. (2010). Shear strength of large concrete members with FRP reinforcement. *Journal of Composites for Construction, 14*(6), 637–646. https://doi.org/10.1061/(ASCE)CC.1943-5614.0000108

Betschoga, C., Tung, N. D., & Tue, N. V. (2021). Investigations on the influence of boundary and loading conditions on the shear resistance of FRP concrete beams without shear reinforcement. *Composite Structures, 262*, Article 113335. https://doi.org/10.1016/j.compstruct.2020.113335

Caporale, A., & Luciano, R. (2009). Indagine sperimentale e numerica sulla resistenza a taglio di travi di calcestruzzo armate con barre di GFRP. *Proceedings of XXXVIII Convegno Nazionale AIAS*.

CEN. (2002). EN1990: Eurocode - Basis of Structural Design, European Commission, Brussels, Belgium.

Chang, K., & Seo, D. (2012). Behavior of one-way concrete slabs reinforced with GFRP bars. *Journal of Asian Architecture and Building Engineering, 11*(2), 351–358. https://doi.org/10.3130/jaabe.11.351

Choi, K.-K., Kim, J. C., & Park, H. G. (2016). Shear Strength Model of Concrete Beams Based on Compression Zone Failure Mechanism. *ACI Structural Journal*. https://doi.org/10.14359/51689032

CSA (Canadian Standard Association). (2021). CSA S806–12: *Design and construction of building structures with fibre-reinforced polymers*. Toronto, ON, Canada: CSA Group.

Deitz, D. H., Harik, I. E., & Gesund, H. (1999). One-way slabs reinforced with glass fiber reinforced polymer reinforcing bars. *Special Publication, 188*, 279–286. https://doi.org/10.14359/5629

Dinh, N. H., Kim, J. C., Lee, S. J., Choi, K. K., & Park, H. G. (2020). Modeling parameters for the nonlinear analysis of reinforced concrete beams under cyclic loading. *Engineering Structures, 216*, Article 110715. https://doi.org/10.1016/j.engstruct.2020.110715

Dinh, N. H., Pham, H. H., Kim, S. H., & Choi, K. K. (2023). Experimental investigation on flexural and direct shear behaviors of specimens made of lightweight carbon textile-reinforced cementitious composites. *Structural Concrete, 24*(4), 5027–5054. https://doi.org/10.1002/suco.202200509

Dinh, N. H., Pham, H. H., Kim, S. H., & Choi, K. K. (2024). Tensile performance and cracking characteristics of sustainable textile-reinforced cementitious composites utilizing expanded glass aggregate and fly ash replacement. *Construction and Building Materials, 425*, Article 136084. https://doi.org/10.1016/j.conbuildmat.2024.136084

Duranovic, N., Pilakoutas, K., & Waldron, P. (1997). Tests on concrete beams reinforced with glass fibre reinforced plastic bars. In *Proceedings of the third international symposium on non-metallic (FRP) reinforcement for concrete structures (FRPRCS-3)* (Vol. 2, pp. 479–86). Japan Concrete Institute.

El Refai, A., & Abed, F. (2016). Concrete contribution to shear strength of beams reinforced with basalt fiber-reinforced bars. *Journal of Composites for Construction, 20*(4), 04015082. https://doi.org/10.1061/(ASCE)CC.1943-5614.0000648

El-Sayed, A., El-Salakawy, E., & Benmokrane, B. (2005). Shear strength of one-way concrete slabs reinforced with fiber-reinforced polymer composite bars. *Journal of Composites for Construction, 9*(2), 147–157. https://doi.org/10.1061/(ASCE)1090-0268(2005)9:2(147

El-Sayed, A. K., El-Salakawy, E. F., & Benmokrane, B. (2006a). Shear strength of FRP-reinforced concrete beams without transverse reinforcement. *ACI Materials Journal, 103*(2), 235. https://doi.org/10.14359/15181

El-Sayed, A. K., El-Salakawy, E. F., & Benmokrane, B. (2006cb). Shear capacity of high-strength concrete beams reinforced with FRP bars. *ACI Materials Journal, 103*(3), 383. https://doi.org/10.14359/15316

El-Sayed, A. K., Soudki, K., & Kling, E. (2009). Flexural behaviour of self-consolidating concrete slabs reinforced with GFRP bars. In *Proceedings of the 9th International Symposium on Fiber Reinforced Polymer Reinforcement for Reinforced Concrete Structures, Sydney, Australia* (pp. 13–15).

Farahmand, F. (1996). Shear Behaviour of Concrete Beams Reinforced with Glass Fibre Reinforced Plastic. *Struct. Eng. Div. Dep. Civ. Geol. Eng. Univ. Manit*, 234–345.

Grace, N., Enomoto, T., Baah, P., & Bebawy, M. (2012). Flexural behavior of CFRP precast prestressed decked bulb T-beams. *Journal of Composites for Construction, 16*(3), 225–234. https://doi.org/10.1061/(ASCE)CC.1943-5614.0000266

Gross, S. P., Dinehart, D. W., Yost, J. R., & Theisz, P. M. (2004). Experimental tests of high-strength concrete beams reinforced with CFRP bars. *Proc., ACMBS-IV*, 1–8.

Guadagnini, M. (2002). *Shear behaviour and design of FRP RC beams* (Doctoral dissertation). University of Sheffield, Dept. of Civil and Structural Engineering, Sheffield, UK.

Guadagnini, M., Pilakoutas, K., & Waldron, P. (2006). Shear resistance of FRP RC beams: Experimental study. *Journal of Composites for Construction, 10*(6), 464–473. https://doi.org/10.1061/(ASCE)1090-0268(2006)10:6(464

Huang, Z., Chen, W., Tran, T. T., Pham, T. M., Hao, H., Chen, Z., & Elchalakani, M. (2021). Experimental and numerical study on concrete beams reinforced with Basalt FRP bars under static and impact loads. *Composite Structures, 263*, Article 113648. https://doi.org/10.1016/j.compstruct.2021.113648

Imjai, T. (2008). *Design and analysis of curved FRP composites as shear reinforcement for concrete structures* (Doctoral dissertation). University of Sheffield, Department of Civil and Structural Engineering.

Issa, M. A., Ovitigala, T., & Ibrahim, M. (2016). Shear behavior of basalt fiber reinforced concrete beams with and without basalt FRP stirrups. *Journal of Composites for Construction, 20*(4), 04015083. https://doi.org/10.1061/(ASCE)CC.1943-5614.0000638

Johnson, D. T. C. (2014). Investigation of glass fibre reinforced polymer (GFRP) bars as internal reinforcement for concrete structures (Master thesis). University of Toronto, University of Toronto.

JSCE (Japan Society of Civil Engineers). (2007). Recommendation for design and construction of concrete structures using continuous fiber reinforcing materials. Concrete Engineering Series 23. Tokyo.

Kara, I. F. (2011). Prediction of shear strength of FRP-reinforced concrete beams without stirrups based on genetic programming. *Advances in Engineering Software, 42*(6), 295–304. https://doi.org/10.1016/j.advengsoft.2011.02.002

Kaszubska, M., Kotynia, R., Barros, J. A., & Baghi, H. (2018). Shear behavior of concrete beams reinforced exclusively with longitudinal glass fiber reinforced polymer bars: Experimental research. *Structural Concrete, 19*(1), 152–161. https://doi.org/10.1002/suco.201700174

Khaja, M. N., & Sherwood, E. G. (2013). Does the shear strength of reinforced concrete beams and slabs depend upon the flexural reinforcement ratio or the reinforcement strain? *Canadian Journal of Civil Engineering, 40*(11), 1068–1081. https://doi.org/10.1139/cjce-2012-0459

Kilpatrick, A. E., & Dawborn, R. (2006). Flexural shear capacity of high strength concrete slabs reinforced with longitudinal GFRP bars. *Proceedings of 2nd International Congress. FIB, Naples, Italy*, 1–10.

Kilpatrick, A. E., & Easden, L. (2005). Shear capacity of GFRP reinforced high strength concrete slabs. Developments in mechanics of structures and materialsIn J. Deeks & H. Hao (Eds.), *a* (Vol. 1, pp. 119–124). Taylor & Francis.

Kim, C. H., & Jang, H. S. (2014). Concrete shear strength of normal and lightweight concrete beams reinforced with FRP bars. *Journal of Composites for Construction, 18*(2), 04013038. https://doi.org/10.1061/(ASCE)CC.1943-5614.0000440

Korea Concrete Institute. (2024). Design code for shear and torsion of concrete structures (KDS 14 20 22), Korea Design Standard (KDS), Ministry of Land, Infrastructure, and Transport of Korea, Seoul, Republic of Korea. (revision draft).

Krall, M. (2014). *Tests on concrete beams with GFRP flexural and shear reinforcements & analysis method for indeterminate strut-and-tie models with brittle reinforcements* (Master's thesis). University of Waterloo.

Kurth, M. (2012). *Zum Querkrafttragverhalten von Betonbauteilen mit Faserverbundkunststoff-Bewehrung (Shear Behaviour of Concrete Members With Fibre Reinforced Polymers as Internal Reinforcement)* (Doctoral dissertation, Rheinisch-Westfälische Technische Hochschule Aachen).

Liu, R. (2011). *Precast concrete bridge deck panels reinforced with glass fiber reinforced polymer bars* (Doctoral dissertation). The University of Utah.

Maranan, G. B., Manalo, A. C., Benmokrane, B., Karunasena, W., Mendis, P., & Nguyen, T. Q. (2018). Shear behaviour of geopolymer-concrete beams

transversely reinforced with continuous rectangular GFRP composite spirals. *Composite Structures, 187*, 454–465. https://doi.org/10.1016/j.compstruct.2017.12.080
Maruyama, K. (1996). Size effect in shear behavior of FRP reinforced concrete beams advanced composite materials in bridges and structures. *CSCE*, 227–234.
Maruyama, K., & Zhao, W. J. (1994). Flexural and shear behaviour of concrete beams reinforced with FRP rods. *Corrosion and corrosion protection of steel in concrete*. Sheffield Academic Press, 1330–1339.
Matta, F., El-Sayed, A. K., Nanni, A., & Benmokrane, B. (2013). Size effect on concrete shear strength in beams reinforced with fiber-reinforced polymer bars. *ACI Structural Journal*. https://doi.org/10.14359/51685747
Michaluk, C. R., Rizkalla, S. H., Tadros, G., & Benmokrane, B. (1998). Flexural behavior of one-way concrete slabs reinforced by fiber reinforced plastic reinforcements. *ACI Structural Journal, 95*(3), 353–365. https://doi.org/10.14359/552
Mohamed, O. A., & Khattab, R. (2017). Review of punching shear behaviour of flat slabs reinforced with FRP bars. In *IOP Conference Series: Materials Science and Engineering* (Vol. 245, No. 3, p. 032064). IOP Publishing. https://doi.org/10.1088/1757-899X/245/3/032064
Morgado, T., Correia, J. R., Moreira, A., Branco, F. A., & Tiago, C. (2015). Experimental study on the fire resistance of GFRP pultruded tubular columns. *Composites Part B: Engineering, 69*, 201–211. https://doi.org/10.1016/j.compositesb.2014.10.005
Mosley, W. H., Bungey, J. H., & Hulse, R. (1999). *Reinforced concrete design*. Macmillan.
Mukhtar, F., & Deifalla, A. (2023). Shear strength of FRP reinforced deep concrete beams without stirrups: Test database and a critical shear crack-based model. *Composite Structures, 307*, Article 116636. https://doi.org/10.1016/j.compstruct.2022.116636
Nakamura, H., & Higai, T. (1995). Evaluation of shear strength of concrete beams reinforced with FRP. *Doboku Gakkai Ronbunshu, 1995*(508), 89–100.
Nguyen, P. D., & Dang, V. H. (2025). Shear strength of FRP-reinforced concrete deep beams: Extension of beam and arch action model based on data-driven analysis. *Structures, 74*, Article 108553. https://doi.org/10.1016/j.istruc.2025.108553
Niewels, J. (2008). *Zum Tragverhalten von Betonbauteilen mit Faserverbundkunststoff-Bewehrung* (Doctoral dissertation, Aachen, Techn. Hochsch., Diss., 2008).
Noël, M., & Soudki, K. (2014). Shear behavior of post-tensioned FRP-reinforced concrete slabs under static and fatigue loading. *Construction and Building Materials, 69*, 186–195. https://doi.org/10.1016/j.conbuildmat.2014.07.066
Okamoto, T., Nagasaka, T., & Tanigaki, M. (1994). Shear capacity of concrete beams using FRP reinforcement. *Journal of Structural and Construction Engineering, 455*(59), 127–136. https://doi.org/10.3130/aijs.59.127_1
Olivito, R. S., & Zuccarello, F. A. (2010). On the shear behaviour of concrete beams reinforced by carbon fibre-reinforced polymer bars: An experimental investigation by means of acoustic emission technique. *Strain, 46*(5), 470–481. https://doi.org/10.1111/j.1475-1305.2009.00699.x
Park, H. G., Choi, K.-K., & Wight, J. K. (2006). Strain-based shear strength model for slender beams without web reinforcement. *ACI Structural Journal, 103*(6), 783. https://doi.org/10.14359/18228
Park, S. H., Dinh, N. H., Kim, S. H., Lee, S. J., & Choi, K. K. (2021). Direct shear behavior of precast panel connections with cast-in-place shear keys using steel fiber-reinforced cementitious mortar (SFRCM). *Structures, 32*, 2130–2142. https://doi.org/10.1016/j.istruc.2021.04.025
Pham, H. H., Dinh, N. H., & Choi, K. K. (2023). Tensile behavior of lightweight carbon textile-reinforced cementitious composites with dispersed fibers. *Construction and Building Materials, 384*, Article 131455. https://doi.org/10.1016/j.conbuildmat.2023.131455
Rahal, K. N. (2023). A unified shear strength equation for slabs and beams longitudinally reinforced with FRP or steel bars based on simplified cracked elastic properties. *Engineering Structures, 297*, Article 116950. https://doi.org/10.1016/j.engstruct.2023.116950
Razaqpur, A. G., Isgor, B. O., Greenaway, S., & Selley, A. (2004). Concrete contribution to the shear resistance of fiber reinforced polymer reinforced concrete members. *Journal of Composites for Construction, 8*(5), 452–460. https://doi.org/10.1061/(ASCE)1090-0268(2004)8:5(452)
Razaqpur, A. G., Shedid, M., & Isgor, B. (2011). Shear strength of fiber-reinforced polymer reinforced concrete beams subject to unsymmetric loading. *Journal of Composites for Construction, 15*(4), 500–512. https://doi.org/10.1061/(ASCE)CC.1943-5614.0000184
Ruan, X., Lu, C., Xu, K., Xuan, G., & Ni, M. (2020). Flexural behavior and serviceability of concrete beams hybrid-reinforced with GFRP bars and steel bars. *Composite Structures, 235*, Article 111772. https://doi.org/10.1016/j.compstruct.2019.111772
Shehata, E., Morphy, R., & Rizkalla, S. (2000). Fibre reinforced polymer shear reinforcement for concrete members: Behaviour and design guidelines. *Canadian Journal of Civil Engineering, 27*(5), 859–872. https://doi.org/10.1139/l00-004
Spadea, S., Orr, J., Nanni, A., & Yang, Y. (2017). Wound FRP shear reinforcement for concrete structures. *Journal of Composites for Construction, 21*(5), 04017026. https://doi.org/10.1061/(ASCE)CC.1943-5614.0000807
Swamy, N., & Aburawi, M. (1997). Structural implications of using GFRP bars as concrete reinforcement. In *Proceedings of 3rd International Symposium, FRPRCS* (Vol. 3, pp. 503–510).
Tarawneh, A. N., Saleh, E. F., Alghossoon, A. M., Almasabha, G. S., Alajarmeh, O. S., Manalo, A., & Benmokrane, B. (2024). Modified shear design model for steel-and fiber-reinforced polymer-reinforced concrete beams. *ACI Structural Journal, 121*(1), 147–158. https://doi.org/10.14359/51739191
Tariq, M., & Newhook, J. P. (2003). Shear testing of FRP reinforced concrete without transverse reinforcement. In *Proceedings, Annual Conference of the Canadian Society for Civil Engineering* (pp. 1330–1339).
Tomlinson, D., & Fam, A. (2015). Performance of concrete beams reinforced with basalt FRP for flexure and shear. *Journal of Composites for Construction, 19*(2), 04014036. https://doi.org/10.1061/(ASCE)CC.1943-5614.0000491
Tureyen, A. K., & Frosch, R. J. (2002). Shear tests of FRP-reinforced concrete beams without stirrups. *ACI Structural Journal, 99*(4), 427–434. https://doi.org/10.14359/12111
Vecchio, F. J., & Collins, M. P. (1986). The modified compression-field theory for reinforced concrete elements subjected to shear. *ACI Journal Proceedings, 83*(2), 219–231. https://doi.org/10.14359/10416
Vijay, P. V., Kumar, S. V., & GangaRao, H. V. S. (1996). Shear and ductility behavior of concrete beams reinforced with GFRP rebars. In *Proceedings of the 2nd International Conference on Advanced Composite Materials in Bridges and Structures, ACMBS-II, Montreal 1996*.
Wakjira, T. G., Al-Hamrani, A., Ebead, U., & Alnahhal, W. (2022). Shear capacity prediction of FRP-RC beams using single and ensemble ExPlainable Machine learning models. *Composite Structures, 287*, Article 115381. https://doi.org/10.1016/j.compstruct.2022.115381
Wegian, F. M., & Abdalla, H. A. (2005). Shear capacity of concrete beams reinforced with fiber reinforced polymers. *Composite Structures, 71*(1), 130–138. https://doi.org/10.1016/j.compstruct.2004.10.001
Xue, W., Peng, F., & Zheng, Q. (2016). Design equations for flexural capacity of concrete beams reinforced with glass fiber–reinforced polymer bars. *Journal of Composites for Construction, 20*(3), 04015069. https://doi.org/10.1061/(ASCE)CC.1943-5614.0000630
Xue, X., Lin, L., Gao, J., & Chen, L. (2025). Enhancing shear strength predictions for FRP-Reinforced concrete beams: Focusing on reasonable assessment of average ultimate strain in stirrups. *Structures, 71*, Article 107900. https://doi.org/10.1016/j.istruc.2024.107900
Yang, F. (2014). *Deformation behaviour of beams reinforced with fibre reinforced polymer bars under bending and shear* (Doctoral dissertation, University of Sheffield).
Yost, J. R., Gross, S. P., & Dinehart, D. W. (2001). Shear strength of normal strength concrete beams reinforced with deformed GFRP bars. *Journal of Composites for Construction, 5*(4), 268–275. https://doi.org/10.1061/(ASCE)1090-0268(2001)5:4(268)
Zeidan, M., Barakat, M. A., Mahmoud, Z., & Khalifa, A. (2011). Evaluation of concrete shear strength for FRP reinforced beams. In *Structures Congress 2011* (pp. 1816–1826). https://doi.org/10.1061/41171(401)158
Zhao, W., Maruyama, K., & Suzuki, H. (1995). Shear behavior of concrete beams reinforced by FRP rods as longitudinal and shear reinforcement. In *Proceedings of the second international RILEM symposium on non-metallic (FRP) Reinforcement for Concrete Structures (FRPRCS-2)* (pp. 352–359).

## Publisher's Note

**Ngoc Hieu Dinh** is a postdoctoral researcher in the School of Architecture at Soongsil University, Korea. He received his MS and PhD degrees in Architectural Engineering from Soongsil University. His research interests include the seismic design of RC structures and application of fiber-reinforced concrete/textile reinforced concrete.

**Si-Hyun Kim** is a Masters student in the School of Architecture at Soongsil University, Korea. He received his BE from the School of Architecture, Soongsil University. His research interests include the design and testing of RC structures.

**Kyoung-Kyu Choi** is a Professor in the School of Architecture at Soongsil University, Korea. He received his BE, MS, and PhD in architectural engineering from the Seoul National University. He was an associate member of Joint ACI – ASCE Committee 445. He received the ACI Chester Paul Siess Award for Excellence in Structural Research in 2009 and 2012. His research interests include the shear and seismic design of RC structures and application of fiber-reinforced concrete.